Supporting information for:

Reactions of Rh(PNP) pincer complexes with terminal alkynes: homocoupling through a ring or not at all

Table of contents

1. General experimental methods

All manipulations were performed under an atmosphere of argon using Schlenk and glove box techniques unless otherwise stated. Glassware was oven dried at 150 °C overnight and flame-dried under vacuum prior to use. Molecular sieves were activated by heating at 300 °C *in vacuo* overnight. 1,2-Difluorobenzene (DFB) was pre-dried over Al_2O_3, distilled from calcium hydride and dried twice over 3 Å molecular sieves. CD_2Cl_2 was freeze-pump-thaw degassed and dried over 3 Å molecular sieves. C_6D_6 was distilled from sodium and stored over 3 Å molecular sieves. Et_2NH was distilled from CaH_2. $SiMe_4$ was distilled from liquid Na/K alloy and stored over a potassium mirror. Other anhydrous solvents were purchased from Acros Organics or Sigma-Aldrich, freeze-pump-thaw degassed and stored over 3 Å molecular sieves. 3,3-dimethylbutyne (HC≡C*t*Bu) and 1,5-cyclooctadiene (COD) were freeze-pump-thaw degassed and stored over 3 Å molecular sieves. [Rh(PNP-*t*Bu)(CCH*t*Bu)][BAr^F_4],[1] *cis*-PNP-14·2BH_3,[2] *trans*-PNP-14,[2] [$Rh(COD)_2$][BAr^F_4],[3] 3,3-dimethylbut-1-yne-d_1 (DC≡C*t*Bu),[4] *E*-*t*BuC≡CCHCH*t*Bu,[5] and [Rh(*trans*-PONOP-14)(C_2H_4)][BAr^F_4][2] were synthesized according to published procedures. All other reagents are commercial products and were used as received. NMR spectra were recorded on Bruker spectrometers under argon at 298 K unless otherwise stated. Chemical shifts are quoted in ppm and coupling constants in Hz. NMR spectra in DFB were recorded using an internal capillary of C_6D_6. High resolution (HR) ESI-MS were recorded on Bruker Maxis Plus instrument. IR spectra were recorded on a Jasco FT-IR-4700 using a KBr transmission cell in CH_2Cl_2. Microanalyses were performed at the London Metropolitan University by Stephen Boyer or Elemental microanalysis Ltd.

2. Reaction of [Rh(PNP-tBu)(CCH*t*Bu)][BAr$^{F}_{4}$] (II) with excess HC≡C*t*Bu

To a solution of **II** (20.4 mg, 14.1 μmol) in DFB (0.5 mL) within a J. Young valve NMR tube was added HC≡C*t*Bu (2.6 μL, 21.1 μmol). The resulting solution was heated at 80 °C for 16 h. Analysis by ^{1}H and ^{31}P NMR spectroscopy indicated no significant reaction had occurred.

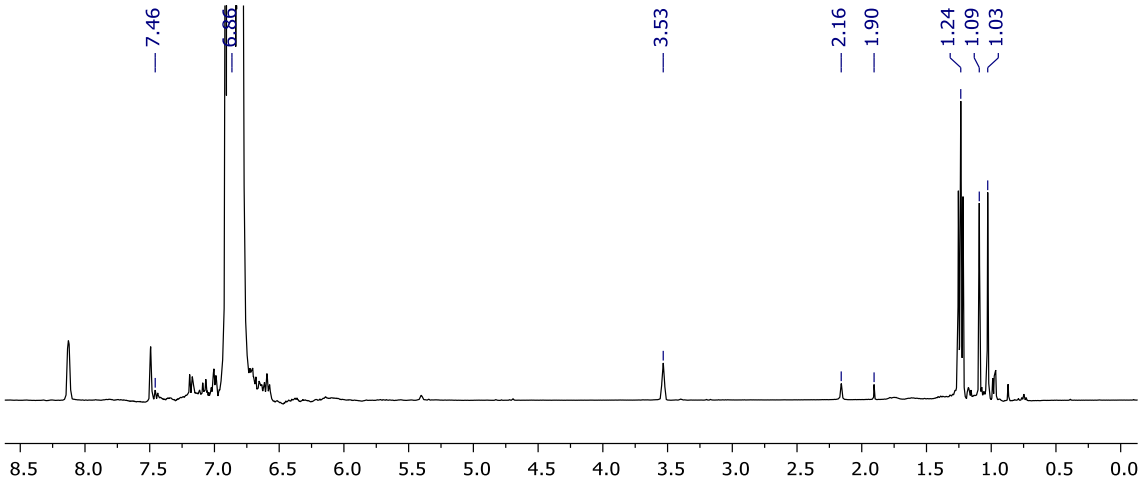

Figure S1. ^{1}H NMR spectrum of the reaction between **II** and excess HC≡C*t*Bu, after heating at 80 °C for 16 h (DFB, 400 MHz).

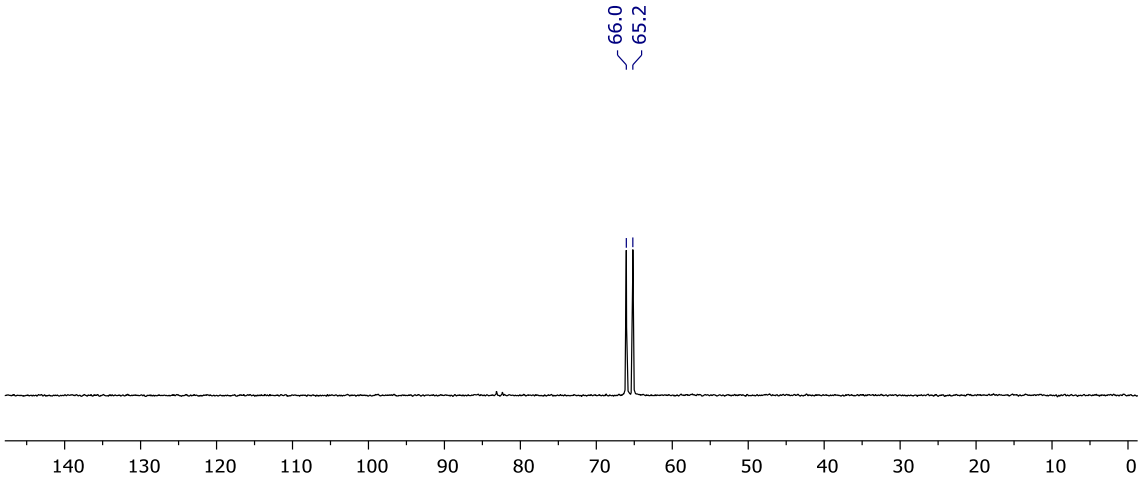

Figure S2. ^{31}P{^{1}H} NMR spectrum of the reaction between **II** and excess HC≡C*t*Bu, after heating at 80 °C for 16 h (DFB, 162 MHz).

3. Deprotection of *cis*-PNP-14·2BH$_3$: preparation of *cis*-PNP-14

A solution of *cis*-PNP-14·2BH$_3$ (5.0 mg, 9.89 μmol) in Et$_2$NH (0.5 mL) was heated at 85 °C for 2 days within a J Young valve NMR tube. Quantitative conversion was observed by ^{1}H and ^{31}P NMR spectroscopy. The volatiles were removed *in vacuo* to afford the product as a colourless oil, which was carried forward without further purification.

^{1}H NMR (500 MHz, C_6D_6): δ 7.08–7.15 (m, 3H, py), 3.07 (d, $^2J_{HH}$ = 13.3, 2H, py$C\underline{H}_2$), 3.01 (d, $^2J_{HH}$ = 13.3, 2H, py$C\underline{H}_2$), 1.57–1.67 (m, 2H, CH_2), 1.22–1.55 (m, 26H, CH_2), 1.02 (d, $^3J_{PH}$ = 11.1, 18H, *t*Bu).
^{13}C{^{1}H} NMR (126 MHz, C_6D_6): δ 160.2 (d, $^2J_{PC}$ = 9, py), 136.1 (s, py), 120.8 (d, $^3J_{PC}$ = 8, py), 35.5 (d, $^1J_{PC}$ = 23, py$\underline{C}H_2$), 30.8 (d, $^3J_{PC}$ = 12, CH_2), 28.3–28.6 (m, 4×CH_2 + *t*Bu{C}), 27.6 (d, $^2J_{PC}$ = 13, *t*Bu{CH_3}), 27.0 (d, $^2J_{PC}$ = 18, CH_2), 24.2 (d, $^1J_{PC}$ = 19, PCH_2).
^{31}P{^{1}H} NMR (121 MHz, C_6D_6): δ 5.9 (s, 2P).

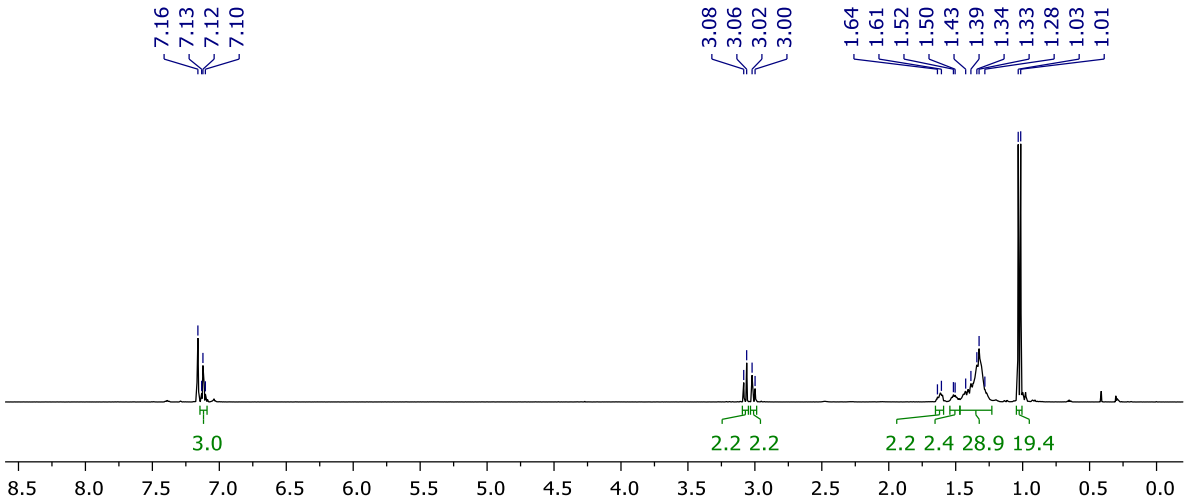

Figure S3. ^{1}H NMR spectrum of *cis*-PNP-14 (C_6D_6, 500 MHz).

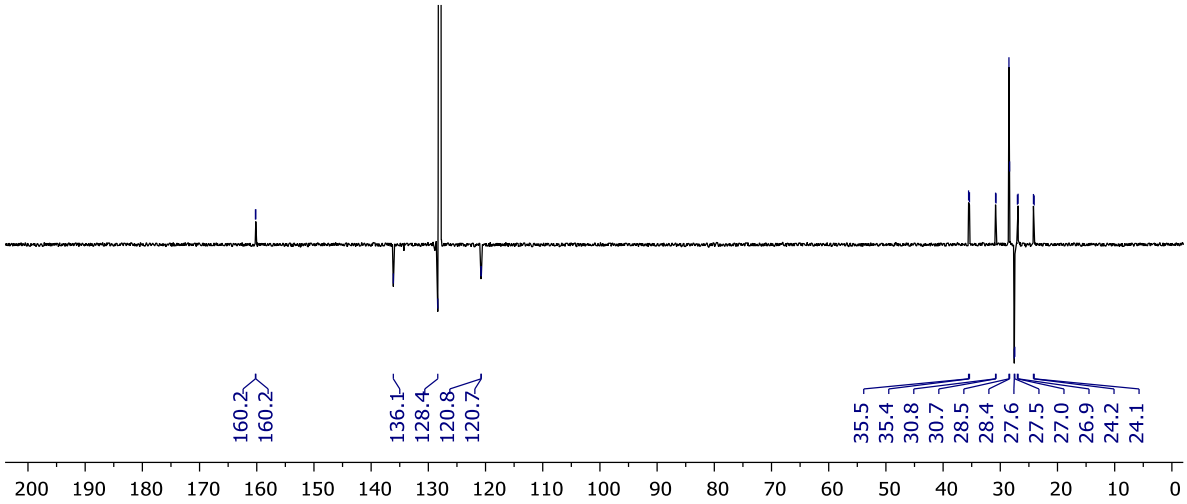

Figure S4. ^{13}C{^{1}H} APT NMR spectrum of *cis*-PNP-14 (C_6D_6, 126 MHz).

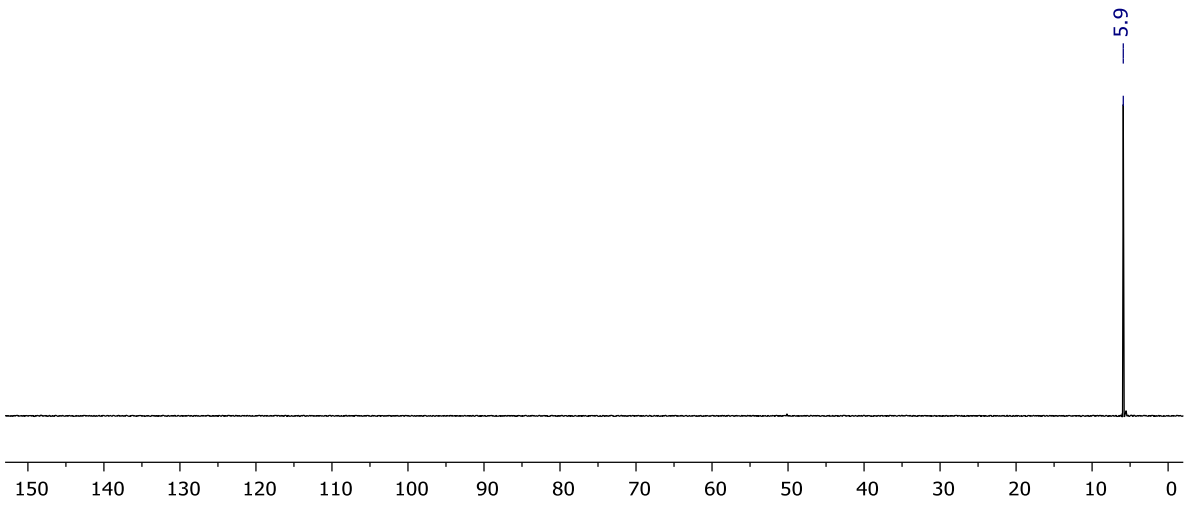

Figure S5. $^{31}P\{^{1}H\}$ NMR spectrum of *cis*-PNP-14 (C_6D_6, 162 MHz).

4. [Rh(PNP-14)(η^2-COD)][BAr$^F_4$] (1′) and [{Rh(PNP-14)}$_2$(μ_2-η^2:η^2-COD)][BAr$^F_4$]$_2$ (1″)

4.1. Reaction between *trans*-PNP-14 and [Rh(COD)$_2$][BAr$^F_4$]

A solution of *trans*-PNP-14 (5.4 mg, 11.3 μmol) and [Rh(COD)$_2$][BAr$^F_4$] (13.3 mg, 11.2 μmol) in DFB (0.5 mL) within a J. Young valve NMR tube was stirred for 5 min at RT. Analysis by ^{1}H and ^{31}P NMR spectroscopy indicated formation **1a′** as the major (>95%) organometallic species alongside liberation of COD into solution.

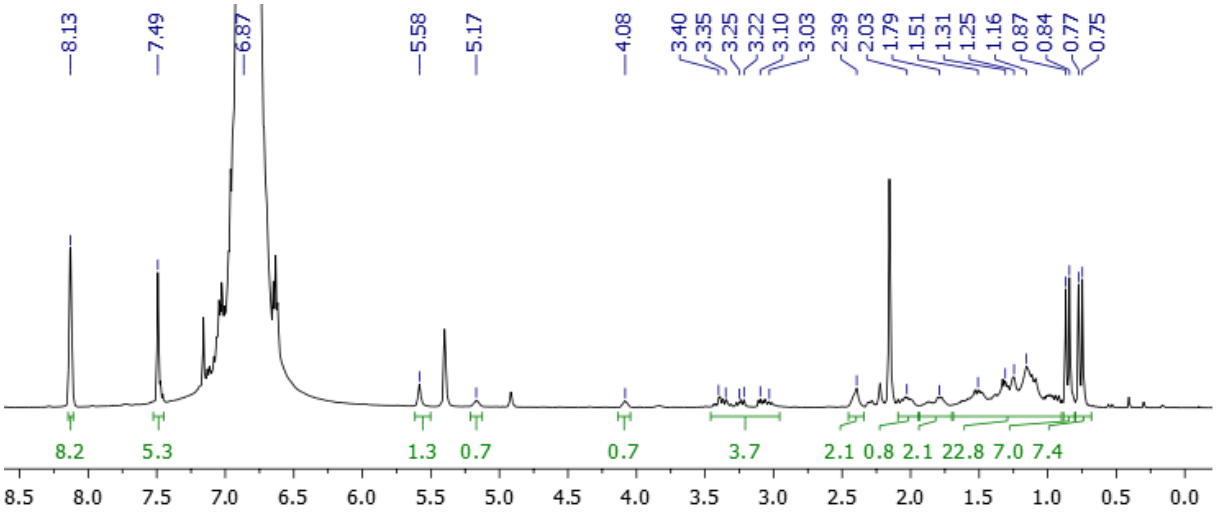

Figure S6. ^{1}H NMR spectrum of the reaction between *trans*-PNP-14 and [Rh(COD)$_2$][BAr$^F_4$] (DFB, 500 MHz).

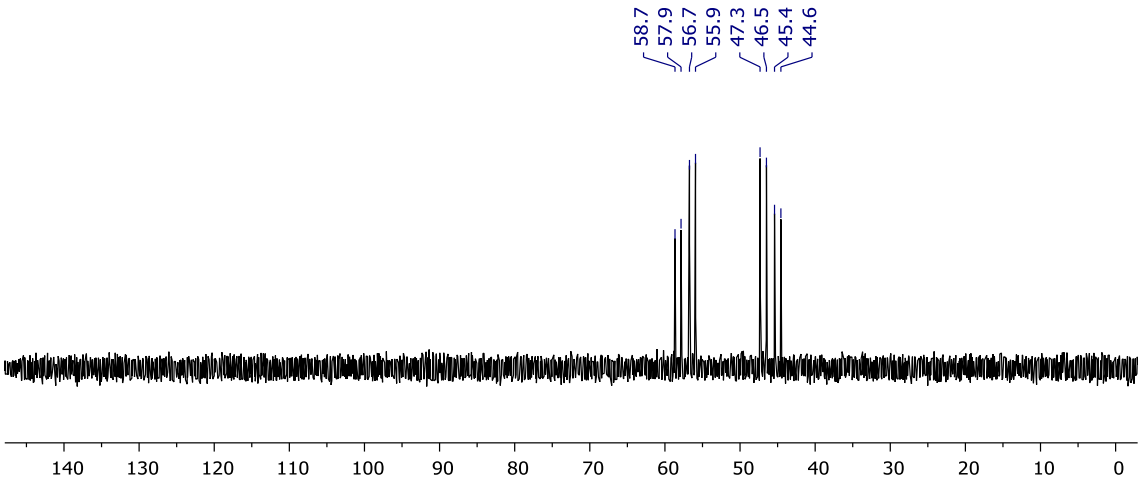

Figure S7. $^{31}P\{^{1}H\}$ NMR of the reaction between *trans*-PNP-14 and $[Rh(COD)_2][BAr^F{}_4]$ (DFB, 162 MHz).

4.2. Characteristion of [Rh(*trans*-PNP-14)(η^2-COD)][$BAr^F{}_4$] (1a′)

A solution of *trans*-PNP-14 (5.4 mg, 11.3 µmol) and $[Rh(COD)_2][BAr^F{}_4]$ (13.3 mg, 11.2 µmol) in DFB (0.5 mL) within a J. Young valve NMR tube was stirred for 5 min at RT and COD (14 µL, 114 µmol) added resulting in the quantitative formation of **1a′**, which was characterised *in situ* by NMR spectroscopy.

^{1}H NMR (500 MHz, DFB, selected data): δ 7.47 (t, $^{3}J_{HH}$ = 7.8, 1H, py), 7.12 (d, $^{3}J_{HH}$ = 7.8, 1H, py), 7.08 (d, $^{3}J_{HH}$ = 7.8, 1H, py), 5.56–5.61 (m, 2H, CH=CH), 5.12–5.22 (m, 1H, Rh(CH=CH)), 4.05–4.12 (m, 1H, Rh(CH=CH)), 3.42 (dd, $^{2}J_{HH}$ = 17.1, $^{2}J_{PH}$ = 6.4, 1H, pyC$\underline{H}_2$), 3.35 (ddd, $^{2}J_{HH}$ = 17.1, $^{2}J_{PH}$ = 13.1, $^{4}J_{PH}$ = 2.6, 1H, pyC$\underline{H}_2$), 3.25 (dd, $^{2}J_{HH}$ = 16.6, $^{2}J_{PH}$ = 10.4, 1H, pyC$\underline{H}_2$), 3.09 (dd, $^{2}J_{HH}$ = 16.9, $^{2}J_{PH}$ = 7.4, 1H, pyC$\underline{H}_2$), 0.86 (d, $^{3}J_{PH}$ = 13.6, 9H, *t*Bu), 0.76 (d, $^{3}J_{PH}$ = 13.5, 9H, *t*Bu).
^{13}C{^{1}H} NMR (126 MHz, DFB): δ 163.2 (obscured, py), 161.1 (d, $^{2}J_{PC}$ = 6, py), 139.2 (s, py), 129.5 (obscured, CH=CH), 120.6 (d, $^{3}J_{PC}$ = 9, py), 120.1 (d, $^{3}J_{PC}$ = 8, py), 81.2 (d, $^{1}J_{RhC}$ = 12, Rh(CH=CH)), 66.9 (d, $^{1}J_{RhC}$ = 10, Rh(CH=CH)), 39.0 (d, $^{1}J_{PC}$ = 21, py$\underline{C}H_2$), 37.4 (d, $^{1}J_{PC}$ = 17, py$\underline{C}H_2$), 33.5 (d, $^{1}J_{PC}$ = 21, *t*Bu{C}), 32.0–32.3 (m, *t*Bu{C}), 27.6 (d, $^{2}J_{PC}$ = 4, *t*Bu{CH_3}), 25.9 (d, $^{2}J_{PC}$ = 6, *t*Bu{CH_3}).
^{31}P{^{1}H} NMR (121 MHz, DFB): δ 57.4 (dd, $^{2}J_{PP}$ = 312, $^{1}J_{RhP}$ = 131, 1P), 45.9 (dd, $^{2}J_{PP}$ = 312, $^{1}J_{RhP}$ = 138, 1P).

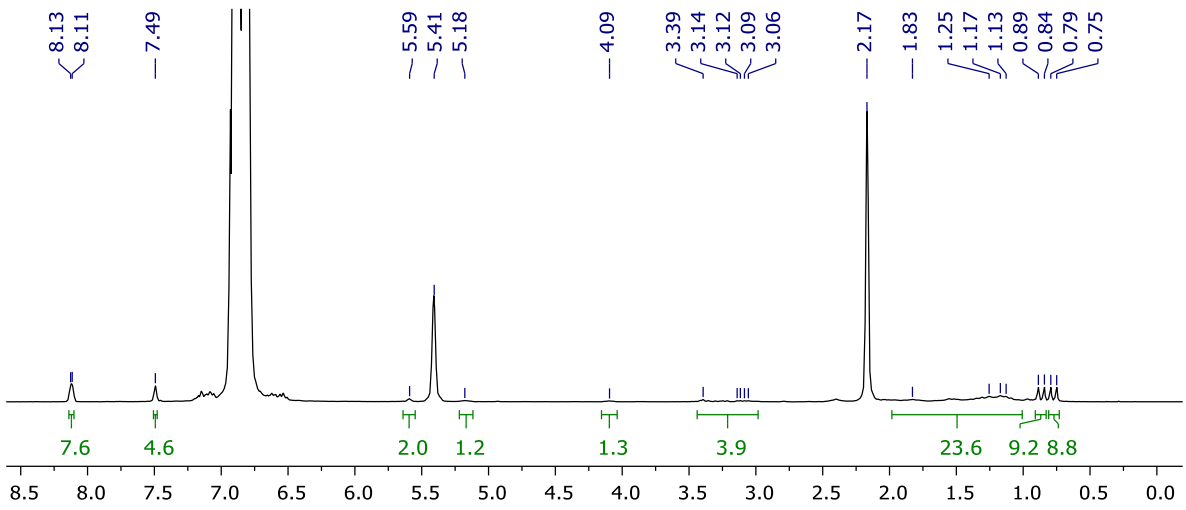

Figure S8. ^{1}H NMR spectrum of **1a′** (DFB, 500 MHz)

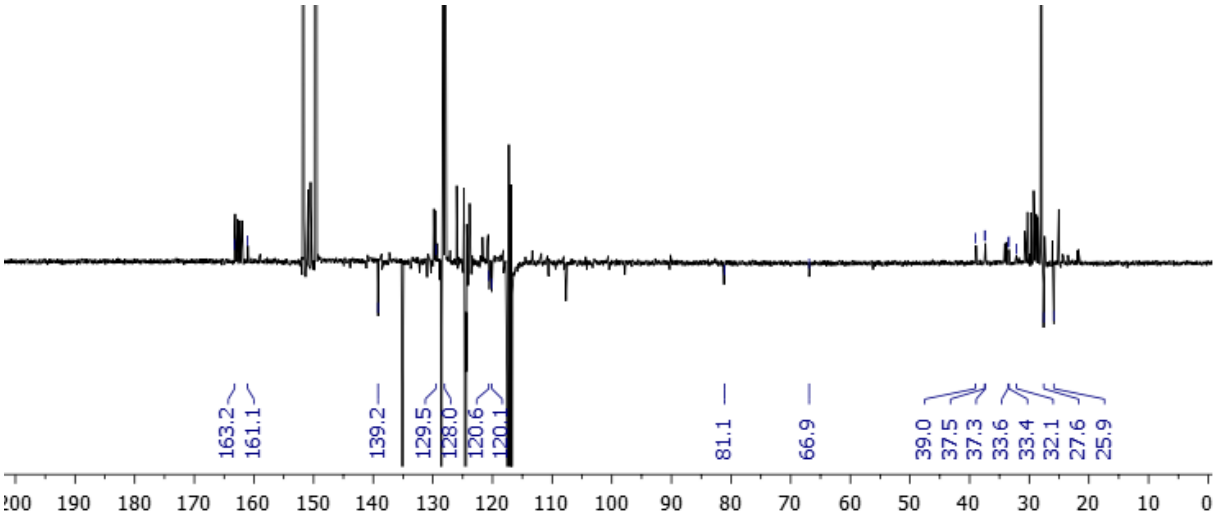

Figure S9. ^{13}C{^{1}H} APT NMR spectrum of **1a′** (DFB, 126 MHz).

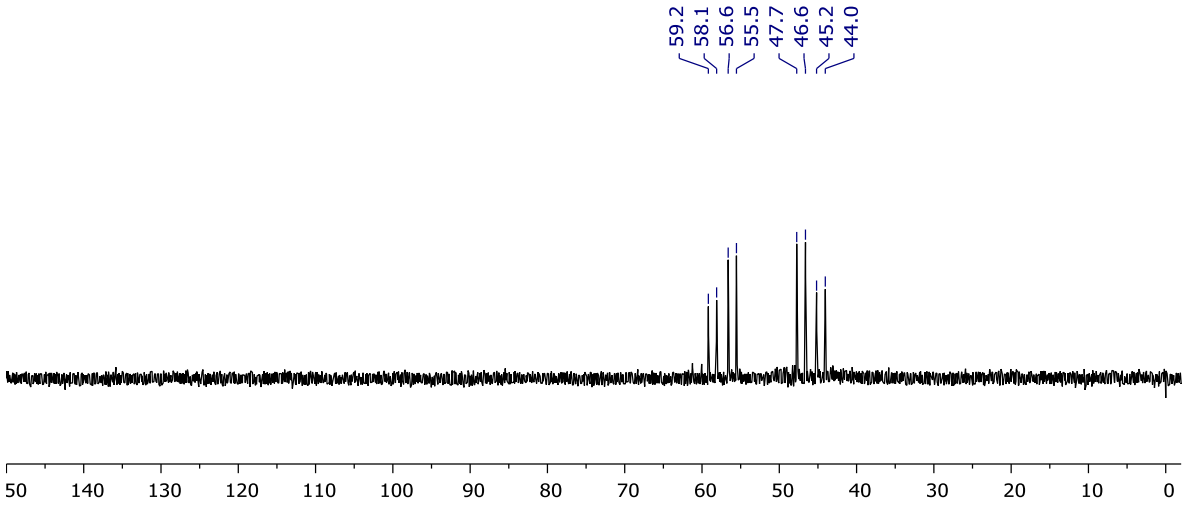

Figure S10. ^{31}P{^{1}H} NMR spectrum of **1a′** (DFB, 121 MHz).

4.3. Isolation and crystal structure of [{Rh(*trans*-PNP-14)}$_2$(μ_2-η^2:η^2-COD)][BAr$^F{}_4$]$_2$ (1a″)

A solution of *trans*-PNP-14 (15.2 mg, 31.8 µmol) and [Rh(COD)$_2$][BAr$^F{}_4$] (37.7 mg, 31.9 µmol) in DFB (0.5 mL) was stirred for 5 min at RT. Volatiles were removed in vacuo and the resulting red oil was washed with pentane (1 mL). The product was obtained as a red crystalline solid by slow diffusion of pentane into an Et_2O solution at -30 °C Yield: 35.4 mg (11.8 µmol, 74%).

Anal. Calcd for $C_{130}H_{142}B_2F_{48}N_2P_4Rh_2$ (2995.8 gmol^{-1}): C, 52.12; H, 4.78; N, 0.94. Found: C, 52.31; H, 4.78; N, 1.02.

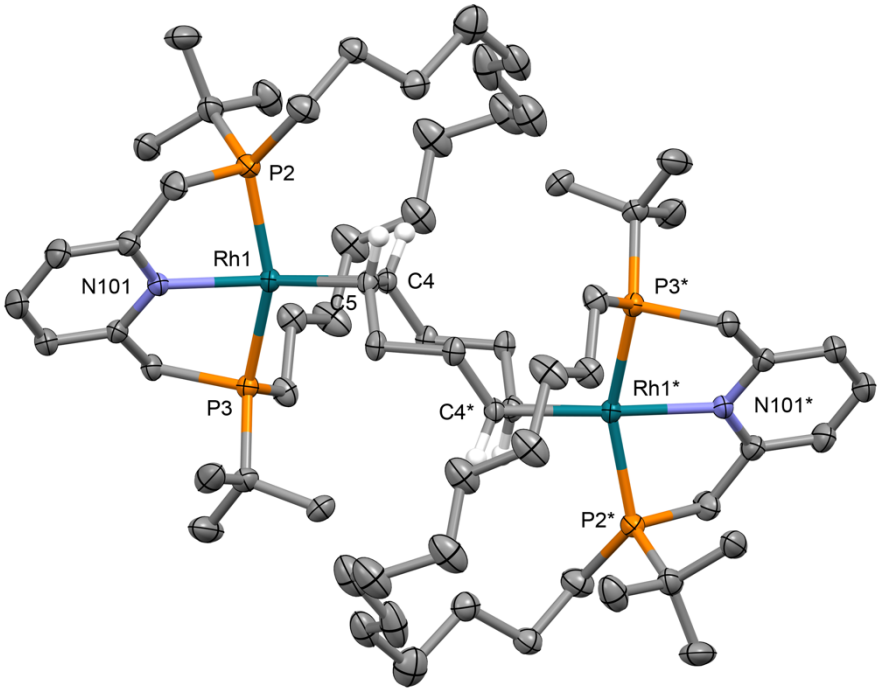

Figure S11. Solid-state structure of **1a″**: thermal ellipsoids drawn at 30% probability, minor disordered component (part of methylene chain), anions, solvent, and most hydrogen atoms omitted. Starred atoms are generated by the symmetry operation: 1–*x*, –*y*, –*z*. Selected bond lengths (Å) and angles (deg): Rh1-P2, 2.2770(12); Rh1-P3, 2.3562(11); Rh1-N101, 2.113(4); P2-Rh1-P3, 155.58(4); Rh1-Cnt(C4,C5), 2.052(3); C4-C5, 1.391(6); N101-Rh1-Cnt(C4,C5), 160.5(2); Cnt = centroid.

4.4. Reaction between *cis*-PNP-14 and [Rh(COD)$_2$][BAr$^F_4$]

A solution of *cis*-PNP-14 (7.0 mg, 14.7 µmol) and [Rh(COD)$_2$][BAr$^F_4$] (17.3 mg, 14.6 µmol) in DFB (0.5 mL) within a J. Young valve NMR tube was stirred for 5 min at RT. Analysis by ^{1}H and ^{31}P NMR spectroscopy indicated formation **1b′** as the major (>95%) organometallic species alongside liberation of COD into solution.

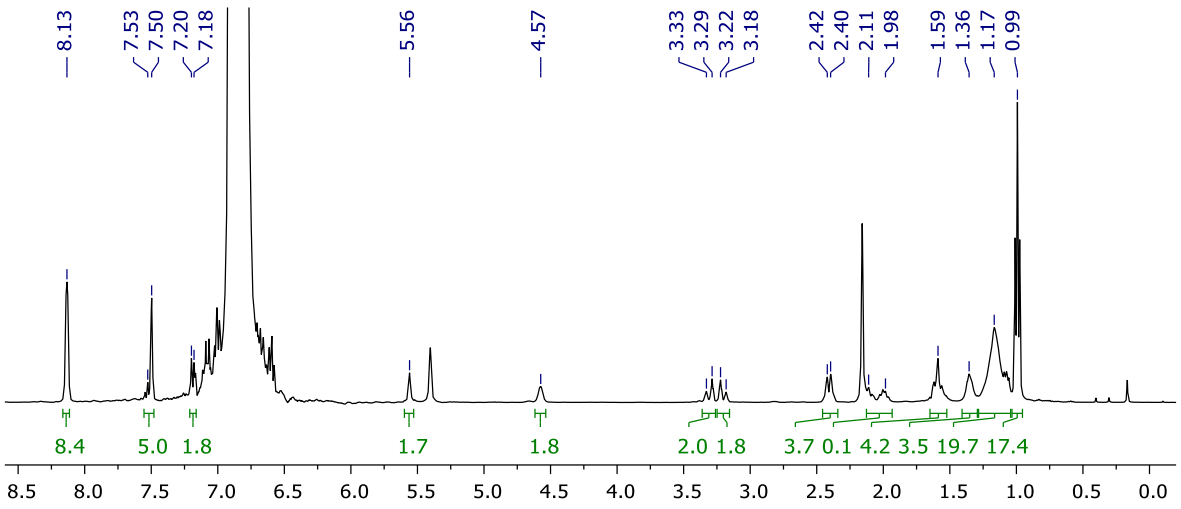

Figure S12. ^{1}H NMR spectrum of the reaction between *cis*-PNP-14 and [Rh(COD)$_2$][BAr$^F_4$] (DFB, 400 MHz).

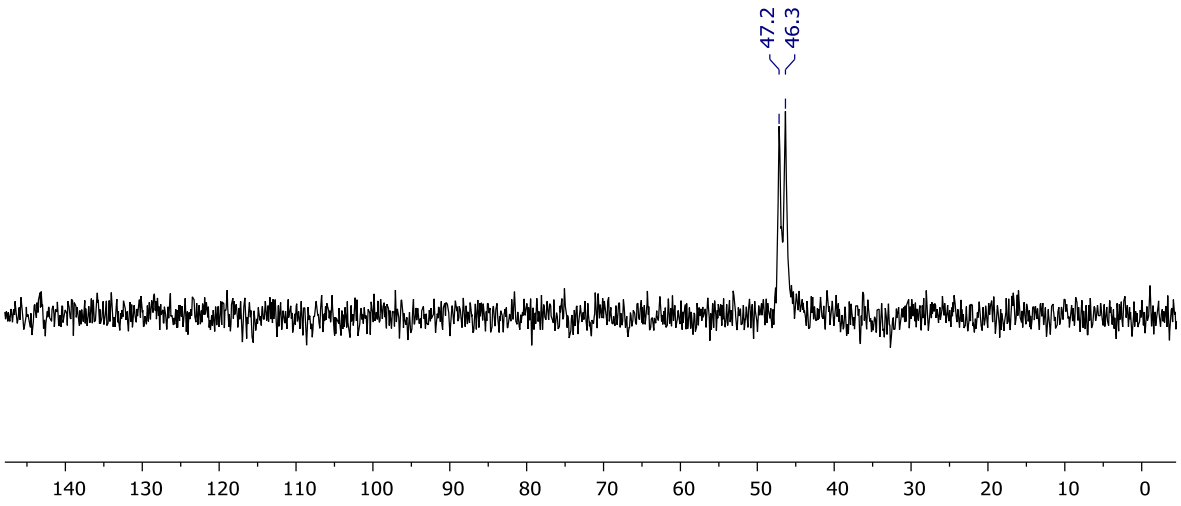

Figure S13. ^{31}P{^{1}H} NMR spectrum of the reaction between *cis*-PNP-14 and [Rh(COD)$_2$][BAr$^F_4$] (DFB, 162 MHz).

4.5. Characterisation of [Rh(*cis*-PNP-14)(η^2-COD)][BAr$^F_4$] (1b′)

A solution of *cis*-PNP-14 (7.0 mg, 14.7 µmol) and [Rh(COD)$_2$][BAr$^F_4$] (17.3 mg, 14.6 µmol) in DFB (0.5 mL) within a J. Young valve NMR tube was stirred for 5 min at RT and COD (18.0 µL, 147 µmol) added resulting in quantitative formation of **1b′**, which was characterised *in situ* by NMR spectroscopy.

^{1}H NMR (500 MHz, DFB, selected data): δ 7.52 (t, $^3J_{HH}$ = 7.8, 1H, py), 7.18 (d, $^3J_{HH}$ = 7.8, 2H, py), 5.56 (t, $^3J_{HH}$ = 3.9, 2H, CH=CH), 4.57 (br, 2H, Rh(CH=CH)), 3.30 (dvt, $^2J_{HH}$ = 17.0, J_{PH} = 3.8, 2H, pyC$\underline{H}_2$), 3.20 (dvt, $^2J_{HH}$ = 17.0, J_{PH} = 3.9, 2H, pyC$\underline{H}_2$), 0.99 (vt, J_{PH} = 7, 18H, *t*Bu).
^{13}C{^{1}H} NMR (126 MHz, DFB, selected data): δ 162.3 (vt, J_{PC} = 3, py), 139.9 (s, py), 129.6 (s, CH=CH), 121.0 (vt, J_{PC} = 9, py), 72.7 (d, $^1J_{RhC}$ = 12, Rh(CH=CH)), 37.3 (vt, J_{PC} = 9, py$\underline{C}H_2$), 32.2 (vt, J_{PC} = 11, *t*Bu{C}), 26.8 (s, *t*Bu{CH$_3$}).
^{31}P{^{1}H} NMR (162 MHz, DFB): δ 46.8 (br d, $^1J_{RhP}$ = 134).

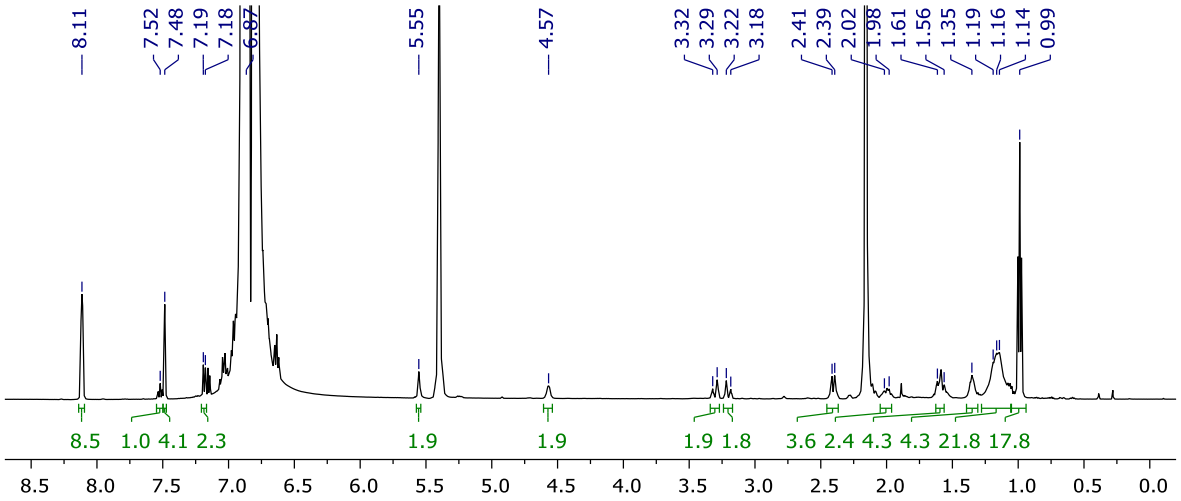

Figure S14. ^{1}H NMR spectrum of **1b′** (DFB, 500 MHz).

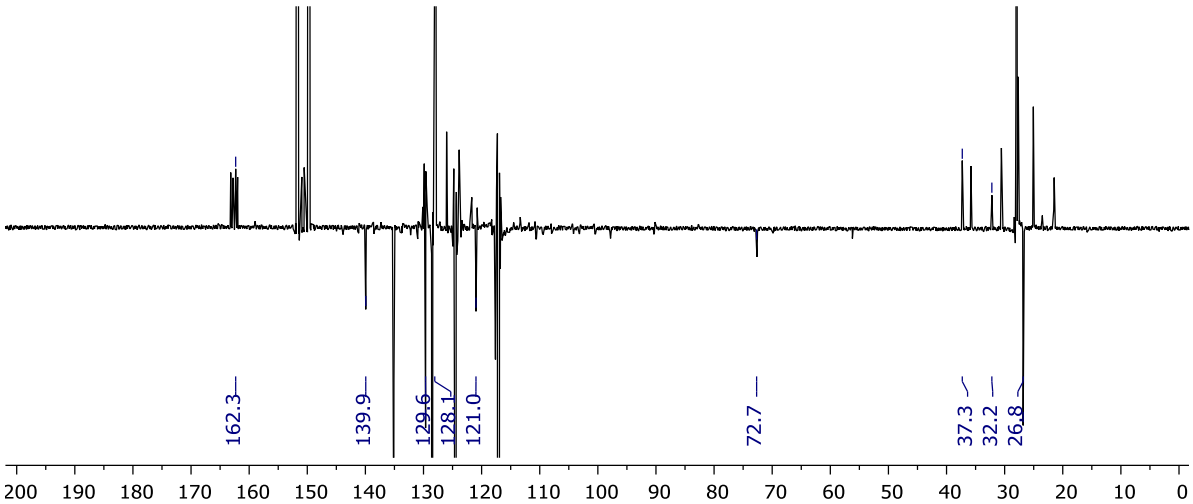

Figure S15. ^{13}C{^{1}H} APT NMR spectrum of **1b′** (DFB, 126 MHz).

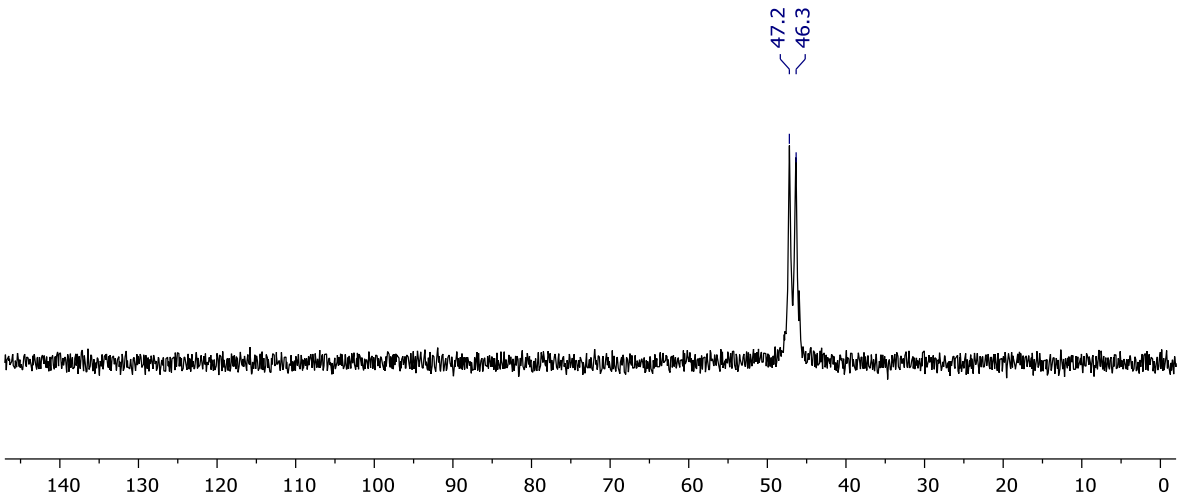

Figure S16. $^{31}P\{^{1}H\}$ NMR spectrum of **1b′** (DFB, 162 MHz).

4.6. Isolation and crystal structure of [{Rh(*cis*-PNP-14)}$_2$(μ_2-η^2:η^2-COD)][BAr$^F{}_4$]$_2$ (1b″)

A solution of *cis*-PNP-14 (10.6 mg, 22.2 µmol) and [Rh(COD)$_2$][BAr$^F{}_4$] (26.2 mg, 22.2 µmol) in DFB (0.5 mL) was stirred for 5 min at RT. Volatiles were removed in vacuo and the resulting red oil was washed with pentane (1 mL). The product was obtained as a red crystalline solid by slow diffusion of pentane into an Et_2O solution at -30 °C. Yield: 28.9 mg (9.65 µmol, 87%).

Anal. Calcd for $C_{130}H_{142}B_2F_{48}N_2P_4Rh_2$ (2995.8 gmol^{-1}): C, 52.12; H, 4.78; N, 0.94. Found: C, 52.03; H, 4.50; N, 1.17.

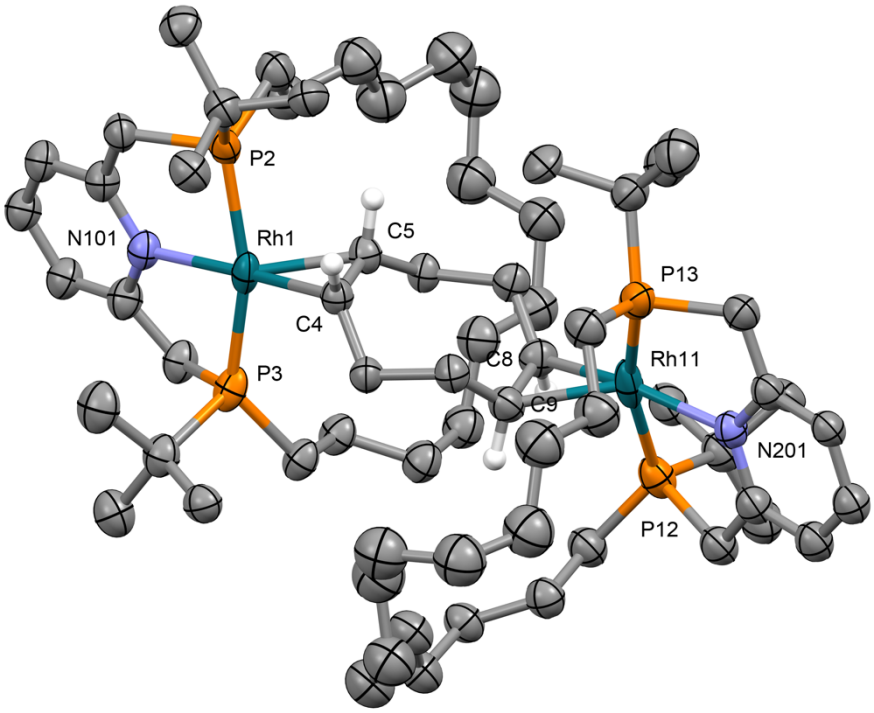

Figure S17. Solid-state structure of **1b″**: thermal ellipsoids drawn at 30% probability, anions and most hydrogen atoms omitted. Low quality data; for establishing connectivity only.

5. Synthesis and reactions of [Rh(*trans*-PNP-14)(CCH*t*Bu)][BAr$^F_4$] (2a)

5.1. Reaction of 1a with HC≡C*t*Bu

A solution of *trans*-PNP-14 (6.1 mg, 12.8 µmol) and [Rh(COD)$_2$][BAr$^F_4$] (15.0 mg, 12.7 µmol) in DFB (0.5 mL) within a J. Young valve NMR tube was mixed for 5 min at RT and HC≡C*t*Bu (4.0 µL, 32.5 µmol) added forming a deep green solution. Analysis by ^{1}H and ^{31}P NMR spectroscopy indicated quantitative formation of **2a**.

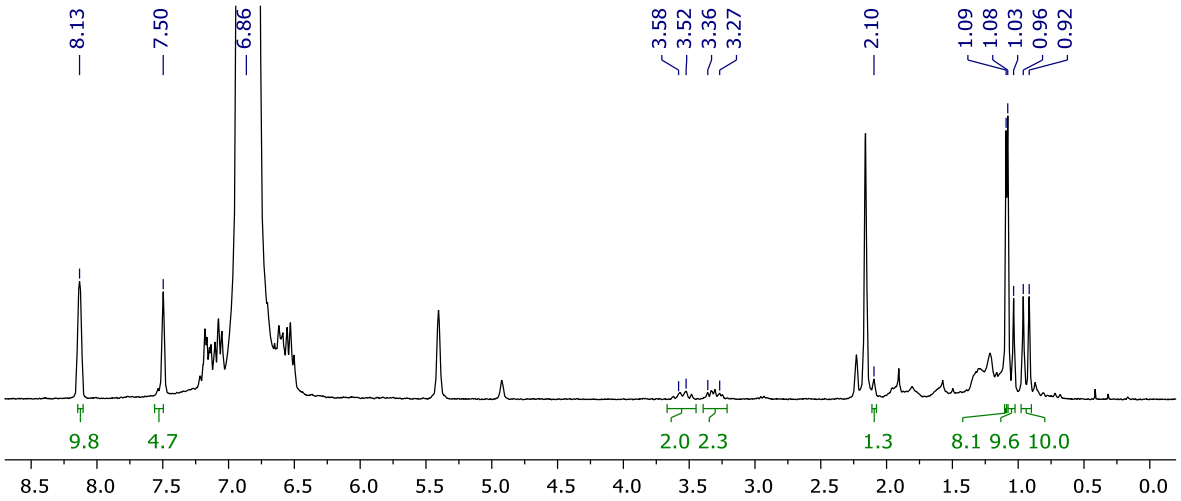

Figure S18. ^{1}H NMR spectrum of the reaction between **1a** and HC≡C*t*Bu (DFB, 300 MHz).

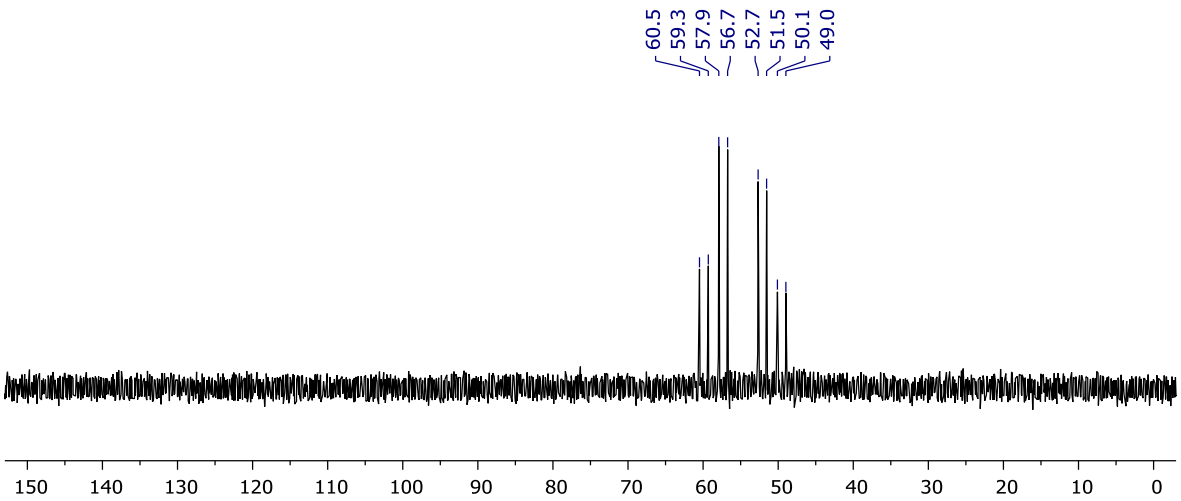

Figure S19. ^{31}P{^{1}H} NMR spectrum of the reaction between **1a** and HC≡C*t*Bu (DFB, 121 MHz).

5.2. Characterisation of 2a *in situ*

A solution of *trans*-PNP-14 (8.3 mg, 17.4 µmol) and [Rh(COD)$_2$][BAr$^F_4$] (20.6 mg, 17.4 µmol) in DFB (0.5 mL) within a J. Young valve NMR tube was mixed for 5 min and HC≡C*t*Bu (10.7 µL, 86.9 µmol) added forming a deep green solution and resulting in quantitative formation of **2a**, which characterised *in situ* by NMR spectroscopy. The presence of excess alkyne in this case increases the solution-phase stability of **2a**, facilitating characterisation.

^{1}H NMR (500 MHz, DFB, selected data): δ 7.50 (obscured, py), 7.20 (d, $^{3}J_{HH}$ = 7.8, 1H, py), 7.15 (d, $^{3}J_{HH}$ = 7.8, 1H, py), 3.48–3.61 (m, 2H, pyC$\underline{H}_2$), 3.25–3.39 (m, 2H, pyC$\underline{H}_2$), 2.09 (s, 1H, CC$\underline{H}$*t*Bu), 1.07 (s, 9H CCH*t*$\underline{Bu}$), 1.05 (d, $^{3}J_{PH}$ = 14.3, 9H, P*t*Bu), 0.93 (d, $^{3}J_{PH}$ = 13.7, 9H, P*t*Bu).

^{13}C{^{1}H} NMR (126 MHz, DFB, selected data): δ 323.7 (partially resolved dt, $^{1}J_{RhC}$ = 57, $^{2}J_{PC}$ not resolved, $\underline{C}$CH*t*Bu), 163 (obscured, py), 141.3 (s, py), 121.1 (d, $^{3}J_{PC}$ = 8, py), 120.8 (d, $^{3}J_{PC}$ = 9, py), 120.5 (dt, $^{2}J_{RhC}$ = 15, $^{3}J_{PC}$ = 5, C$\underline{C}$H*t*Bu), 39.2 (d, $^{1}J_{PC}$ = 19, py$\underline{C}H_2$), 36.5 (d, $^{1}J_{PC}$ = 17, py$\underline{C}H_2$), 28.3 (d, $^{2}J_{PC}$ = 5, P*t*Bu{CH_3}), 26.6 (d, $^{2}J_{PC}$ = 5, P*t*Bu{CH_3}).

^{31}P{^{1}H} NMR (121 MHz, DFB): δ 58.6 (dd, $^{2}J_{PP}$ = 312, $^{1}J_{RhP}$ = 142, 1P), 50.8 (dd, $^{2}J_{PP}$ = 312, $^{1}J_{RhP}$ = 137, 1P).

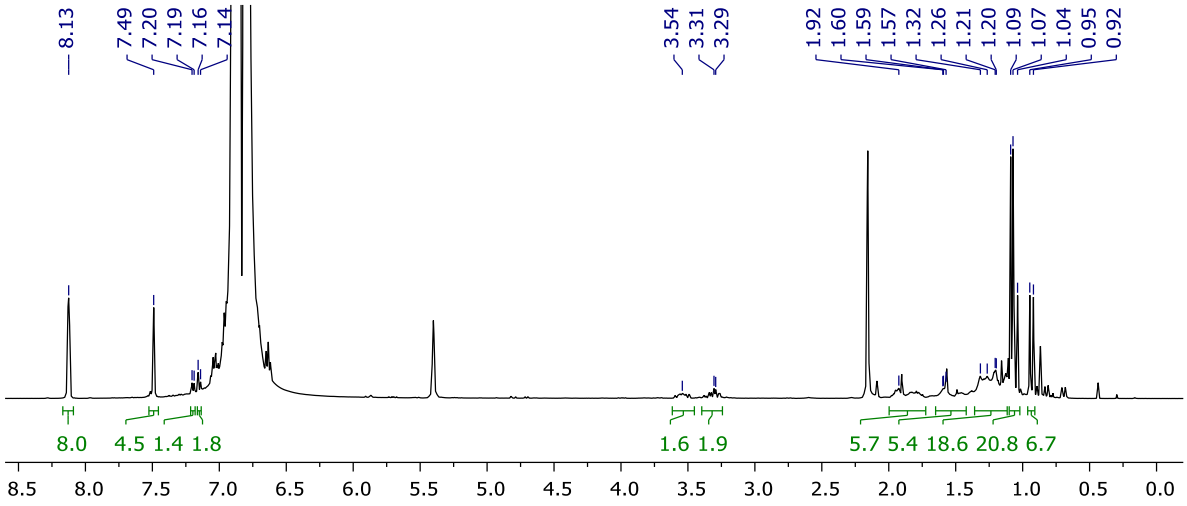

Figure S20. ^{1}H NMR spectrum of **2a** (DFB, 500 MHz).

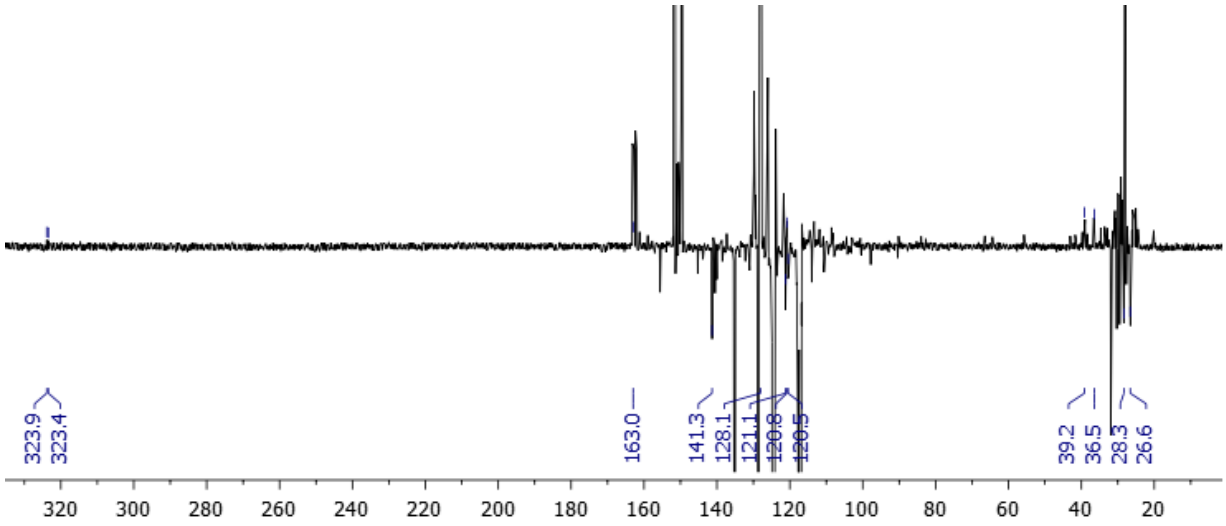

Figure S21. ^{13}C{^{1}H} APT NMR spectrum of **2a** (DFB, 126 MHz).

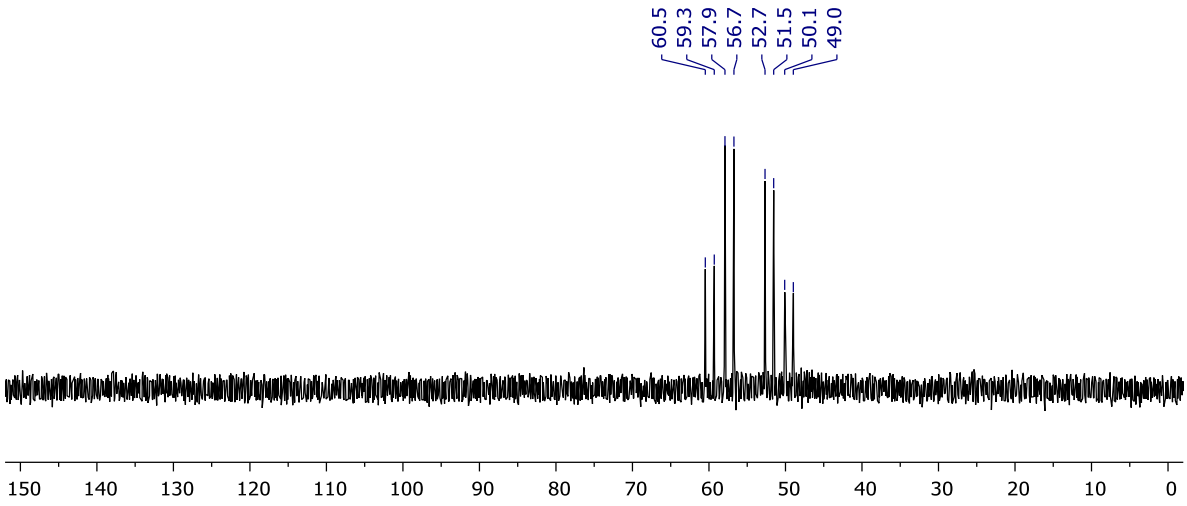

Figure S22. $^{31}P\{^{1}H\}$ NMR spectrum of **2a** (DFB, 121 MHz).

5.3. Reaction of 2a with excess HC≡C*t*Bu

A solution of **2a** in DFB (0.5 mL) with excess HC≡C*t*Bu (1.5 equiv.) within a J. Young valve NMR tube was prepared as described above using *trans*-PNP-14 (8.2 mg, 17.2 μmol), $[Rh(COD)_2][BAr^F{}_4]$ (20.3 mg, 17.2 μmol) and HC≡C*t*Bu (5.3 μL, 43.0 μmol). The solution was heated at 80 °C for 16 h forming a yellow solution. Analysis by ^{1}H and ^{31}P NMR spectroscopy indicated quantitative formation of **3a**.

^{1}H NMR (400 MHz, DFB, selected data): *δ* 7.52 (t, $^{3}J_{HH}$ = 7.8, 1H, py), 7.36 (d, $^{3}J_{HH}$ = 15.5, 1H, CH=C<u>H</u>*t*Bu), 5.89 (d, $^{3}J_{HH}$ = 15.5, 1H, C<u>H</u>=CH*t*Bu), 3.33–3.43 (m, 3H, pyC<u>H</u>$_2$), 3.24 (dd, $^{2}J_{HH}$ = 15.9, $^{2}J_{PH}$ = 9.5, 1H, pyC<u>H</u>$_2$), 1.57 (s, 9H, C≡C*t*Bu), 1.11 (s, 9H, CH=CH*t*<u>Bu</u>), 0.82 (d, $^{3}J_{PH}$ = 12.5, 9H, P*t*Bu), 0.70 (d, $^{3}J_{HH}$ = 12.4, 9H, P*t*Bu).

$^{31}P\{^{1}H\}$ NMR (162 MHz, DFB): *δ* 56.6 (dd, $^{2}J_{PP}$ = 393, $^{1}J_{RhP}$ = 133, 1P), 51.0 (dd, $^{2}J_{PP}$ = 392, $^{1}J_{RhP}$ = 129, 1P).

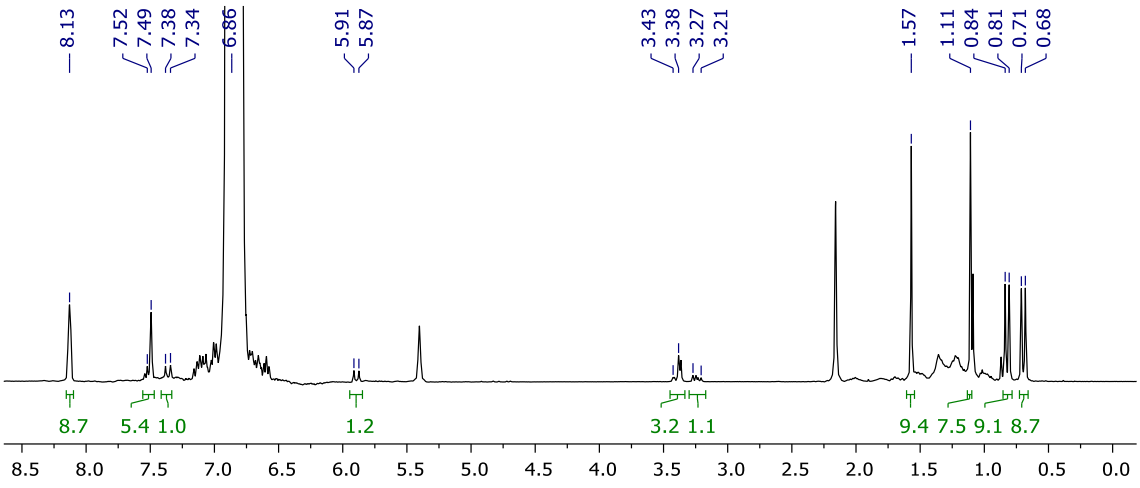

Figure S23. ^{1}H NMR spectrum of the reaction between **1a** and excess HC≡C*t*Bu, after heating at 80 °C for 16 h (DFB, 400 MHz).

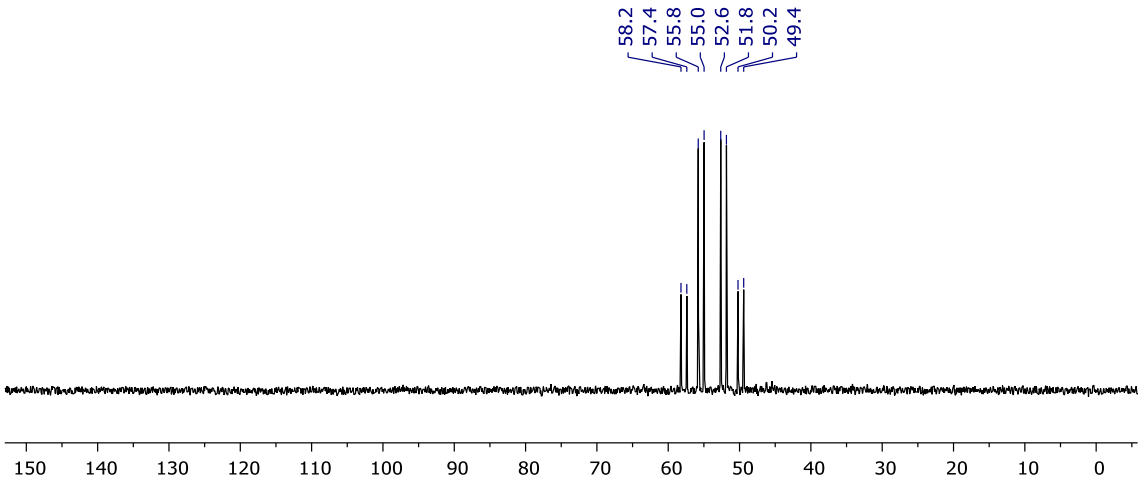

Figure S24. $^{31}P\{^{1}H\}$ NMR spectrum of the reaction between **1a** and excess HC≡C*t*Bu, after heating at 80 °C for 16 h (DFB, 162 MHz).

5.4. Reaction of 2a with excess DC≡C*t*Bu

A solution of **2a** in DFB (0.5 mL) within a J. Young valve NMR tube was prepared as described above using *trans*-PNP-14 (6.6 mg, 13.8 μmol), $[Rh(COD)_2][BAr^F{}_4]$ (16.4 mg, 13.9 μmol) and HC≡C*t*Bu (1.9 μL, 15.4 μmol). To this solution DC≡C*t*Bu (17.0 μL, 136 μmol) was added and the resulting solution heated at 80 °C for 16 h. Volatiles were removed under vacuum, the residue washed with $SiMe_4$, and then analysed by ^{1}H NMR spectrposcopy and HR ESI-MS, with both indicating 83% D incorporation into the enyne core.

^{1}H NMR (500 MHz, CD_2Cl_2, selected data): *δ* 7.40–7.42 (m, 0.18H, CX=C<u>H</u>*t*Bu), 5.95–6.00 (m, 0.17H, C<u>H</u>=CX*t*Bu).

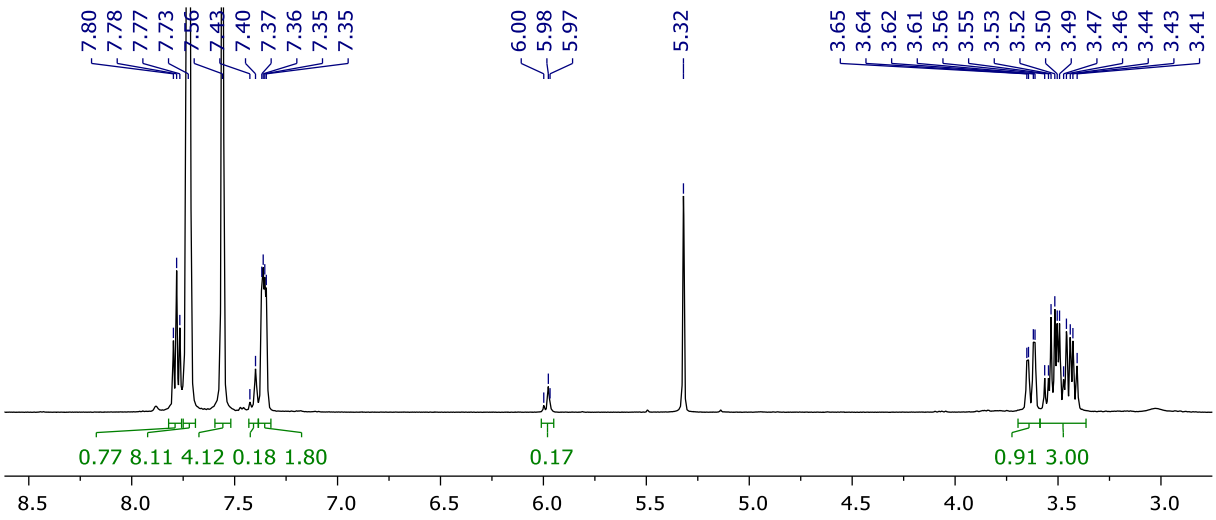

Figure S25. ^{1}H NMR spectrum of the reaction between **2a** and DC≡C*t*Bu (CD_2Cl_2, 500 MHz).

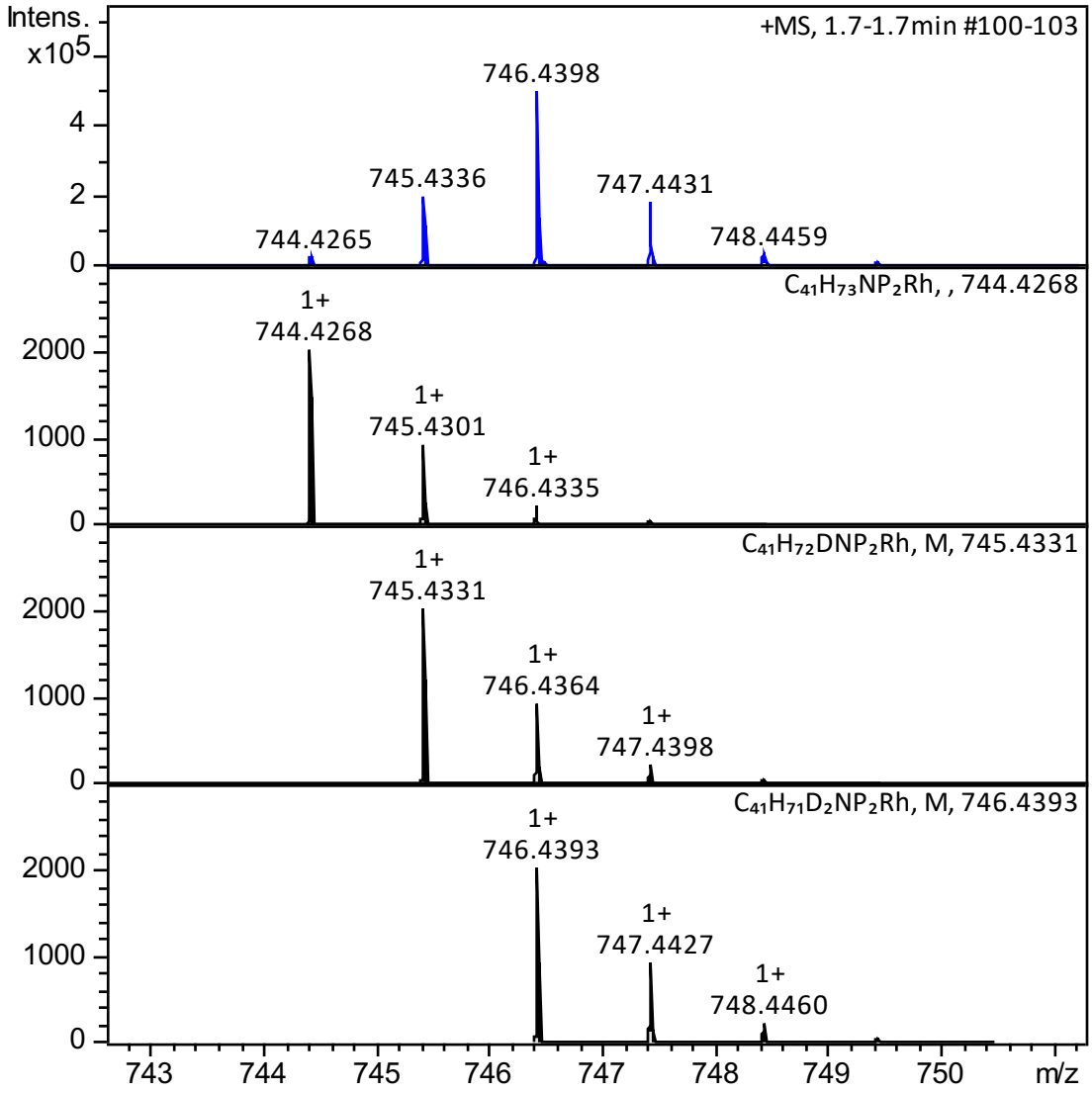

Figure S26. HR ESI-MS of the reaction between **2a** and DC≡C*t*Bu. Fitting gives 3.1% $[d_0\text{-}M]^+$, 23.5% $[d_1\text{-}M]^+$, and 73.4% $[d_2\text{-}M]^+$.

5.5. Reaction of 2a with CO

A solution of **2a** in DFB (0.5 mL) within a J. Young valve NMR tube was prepared as described above using *trans*-PNP-14 (4.3 mg, 9.0 µmol), $[Rh(COD)_2][BAr^F{}_4]$ (10.6 mg, 8.96 µmol) and HC≡C*t*Bu (1.2 µL, 9.74 µmol). This solution was freeze-pump-thaw degassed and placed under an atmosphere of carbon monoxide (1 atm). Analysis by ^1H and ^{31}P NMR spectroscopy indicated quantitative formation of **4a** and liberation of free alkyne within 30 min, by comparison to literature values for the complex.[2]

$^{31}P\{^1H\}$ NMR (162 MHz, DFB): δ 67.0 (d, $^1J_{RhP}$ = 122).

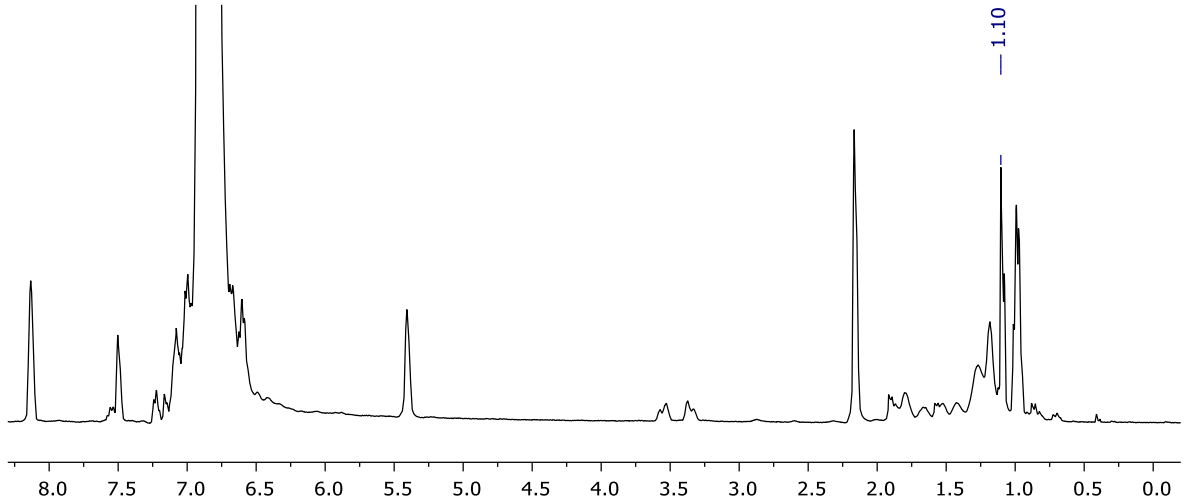

Figure S27. ^{1}H NMR spectrum of the reaction between **2a** and carbon monoxide (DFB, 400 MHz).

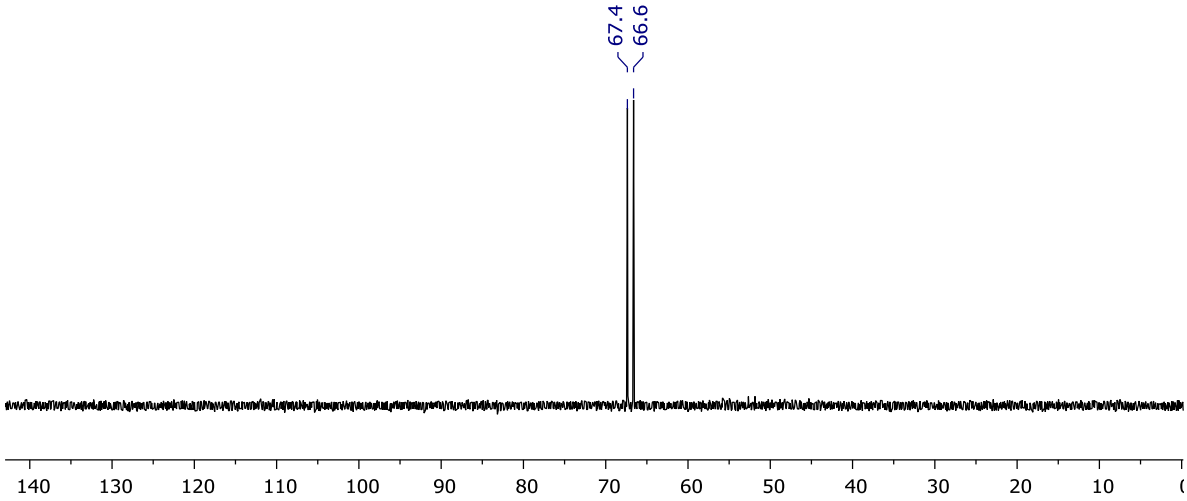

Figure S28. ^{31}P{^{1}H} NMR spectrum of the reaction between **2a** and carbon monoxide (DFB, 162 MHz).

5.6. Preparation of 4a from 1a

A solution of *trans*-PNP-14 (8.3 mg, 17.4 μmol) and $[Rh(COD)_2][BAr^F_4]$ (20.6 mg, 17.4 μmol) in DFB (0.5 mL) within a J. Young valve NMR tube was mixed for 5 min at RT and then freeze-pump-thaw degassed and placed under an atmosphere of carbon monoxide (1 atm). Analysis by ^{1}H and ^{31}P NMR spectroscopy indicated quantitative formation of **4a** within 5 mins, by comparison to literature values for this complex.[2]

^{31}P{^{1}H} NMR (121 MHz, DFB): δ 67.0 (d, $^{1}J_{RhP}$ = 122).

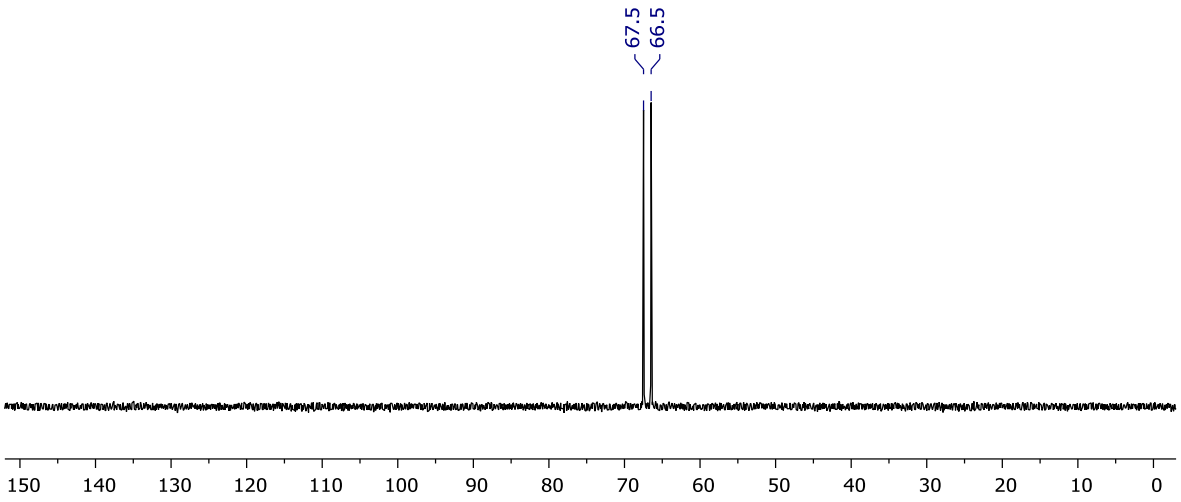

Figure S29. $^{31}P\{^{1}H\}$ NMR spectrum of the reaction between **1a** and carbon monoxide (DFB, 121 MHz).

6. Synthesis, isolation and reactions of [Rh(*cis*-PNP-14)(CCH*t*Bu)][BAr^F_4] (2b)

6.1. Reaction of 1b with HC≡C*t*Bu

A solution of *cis*-PNP-14 (4.8 mg, 10.0 µmol) and $[Rh(COD)_2][BAr^F_4]$ (11.9 mg, 10.1 µmol) in DFB (0.5 mL) within a J. Young valve NMR tube was mixed for 5 min at RT and HC≡C*t*Bu (3.0 µL, 24.4 µmol) added. Analysis by ^{1}H and ^{31}P NMR spectroscopy after 42 h indicated quantitative formation of **2b**.

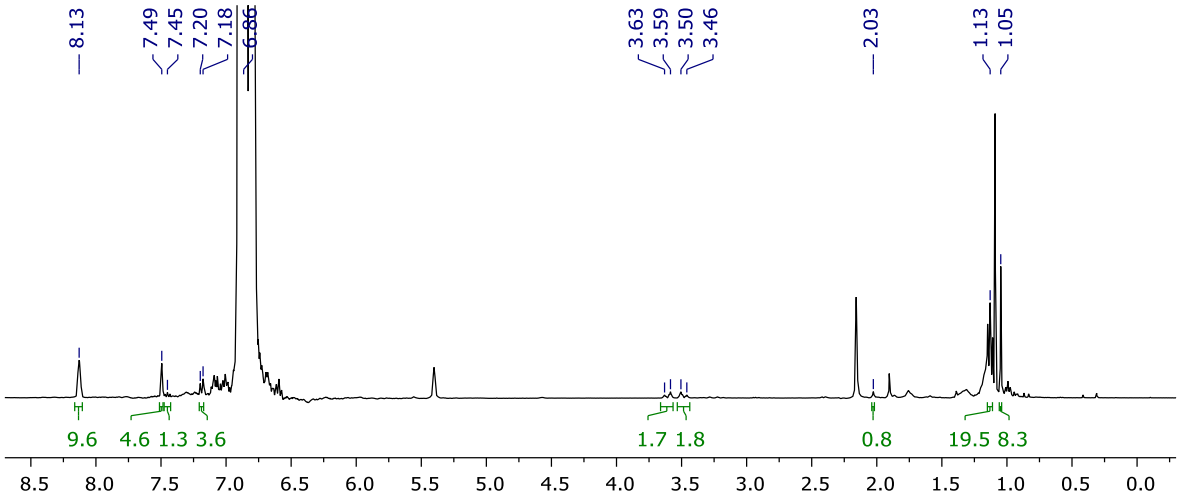

Figure S30. ^{1}H NMR spectrum of the reaction between **1b** and HC≡C*t*Bu (DFB, 400 MHz).

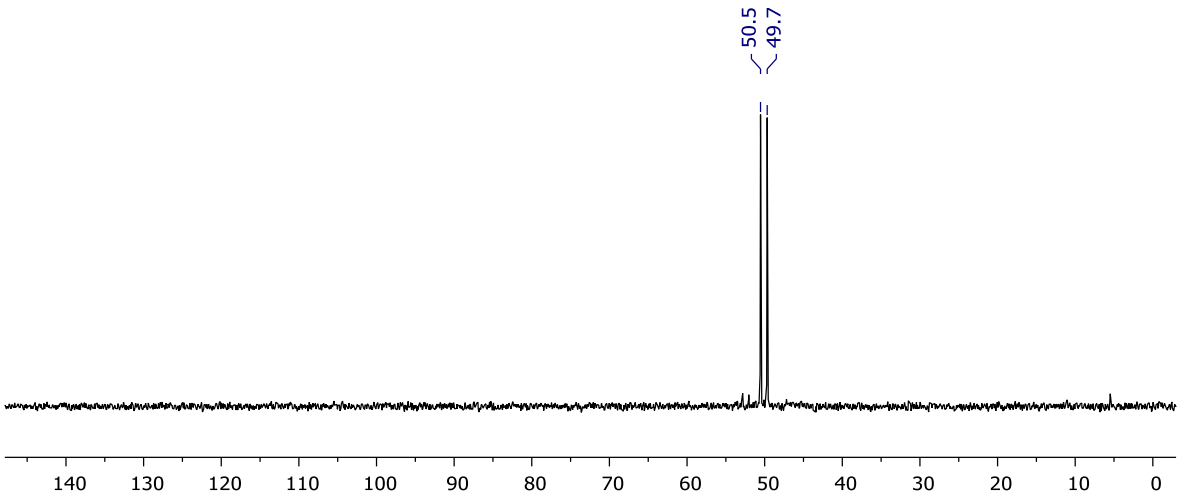

Figure S31. $^{31}P\{^{1}H\}$ NMR spectrum of the reaction between **1b** and **HC≡C*t*Bu** (DFB, 162 MHz).

6.2. Isolation and characterisation of 2b

A solution of *cis*-PNP-14 (4.5 mg, 9.42 µmol) and $[Rh(COD)_2][BAr^F_4]$ (11.1 mg, 9.38 µmol) in DFB (0.5 mL) was mixed for 5 min at RT and HC≡C*t*Bu (5.7 µL, 46.2 µmol) added. The resulting solution was heated at 80 °C for 30 min affording a deep blue solution. Volatiles were removed in vacuo and the resulting blue oil was washed with $SiMe_4$ (1 mL). Recrystallisation by slow diffusion of $SiMe_4$ into an Et_2O solution at 4 ºC afforded the product was a dark purple crystalline solid. Yield: 12.9 mg (8.45 µmol, 90%).

^{1}H NMR (500 MHz, CD_2Cl_2): *δ* 7.70–7.77 (m, 9H, py + Ar^F), 7.56 (br, 4H, Ar^F), 7.40 (d, $^{3}J_{HH}$ = 7.8, 2H, py), 3.77 (dvt, $^{2}J_{HH}$ = 18.1, J_{PH} = 4.0, 2H, pyC<u>H</u>$_2$), 3.67 (dvt, $^{2}J_{HH}$ = 18.1, J_{PH} = 4.2, 2H, pyC<u>H</u>$_2$), 2.18 (s, 1H, CC<u>H</u>*t*Bu), 1.73–2.07 (m, 6H, CH_2), 1.03–1.57 (m, 22H, CH_2), 1.27 (vt, J_{PH} = 8, 18H, P*t*Bu), 1.13 (s, 9H, CCH<u>*t*Bu</u>).

^{1}H NMR (500 MHz, DFB, selected data): *δ* 7.45 (t, $^{3}J_{HH}$ = 7.8, 1H, py), 7.19 (d, $^{3}J_{HH}$ = 7.8, 2H, py), 3.60 (dvt, $^{2}J_{HH}$ = 18.1, J_{PH} = 4.1, 2H, pyC<u>H</u>$_2$), 3.48 (dvt, $^{2}J_{HH}$ = 18.1, J_{PH} = 4.2, 2H, pyC<u>H</u>$_2$), 2.03 (s, 1H, CC<u>H</u>*t*Bu), 1.13 (vt, J_{PH} = 8, P*t*Bu), 1.05 (s, CCH<u>*t*Bu</u>).

^{13}C{^{1}H} NMR (126 MHz, CD_2Cl_2): *δ* 328.9 (dt, $^{1}J_{RhC}$ = 53, $^{2}J_{PC}$ = 15, <u>C</u>CH*t*Bu), 164.4 (vtd, J_{PC} = 5, $^{2}J_{RhC}$ = 1, py), 162.3 (q, $^{1}J_{CB}$ = 50, Ar^F), 141.3 (s, py), 135.4 (s, Ar^F), 129.4 (qq, $^{2}J_{FC}$ = 32, $^{3}J_{CB}$ = 3, Ar^F), 125.1 (q, $^{1}J_{FC}$ = 272, Ar^F), 122.1 (vt, J_{PC} = 5, py), 121.0 (dt, $^{2}J_{RhC}$ = 15, $^{3}J_{PC}$ = 4, C<u>C</u>H*t*Bu), 118.0 (sept, $^{3}J_{FC}$ = 4, Ar^F), 38.3 (vt, J_{PC} = 9, py<u>C</u>H$_2$), 33.0 (vtd, J_{PC} = 13, $^{2}J_{RhC}$ = 2, P*t*Bu{C}), 32.7 (s, CCH<u>*t*Bu</u>{CH_3}), 31.4 (vt, J_{PC} = 8, CH_2), 30.0 (s, CCH<u>*t*Bu</u>{C}), 28.9 (s, CH_2), 27.9 (s, CH_2), 27.7 (s, CH_2), 27.4 (vt, J_{PC} = 3, P*t*Bu{CH_3}), 26.9 (s, CH_2), 26.7 (s, CH_2), 22.8 (vtd, J_{PC} = 11, $^{2}J_{RhC}$ = 3, P<u>C</u>H$_2$).

^{31}P{^{1}H} NMR (121 MHz, CD_2Cl_2): *δ* 50.7 (d, $^{1}J_{RhP}$ = 139).

^{31}P{^{1}H} NMR (162 MHz, DFB): *δ* 50.1 (d, $^{1}J_{RhP}$ = 139).

HR ESI-MS (positive ion 4 kV): 662.3487 ($[M]^+$, calcd 662.3485) *m/z*.

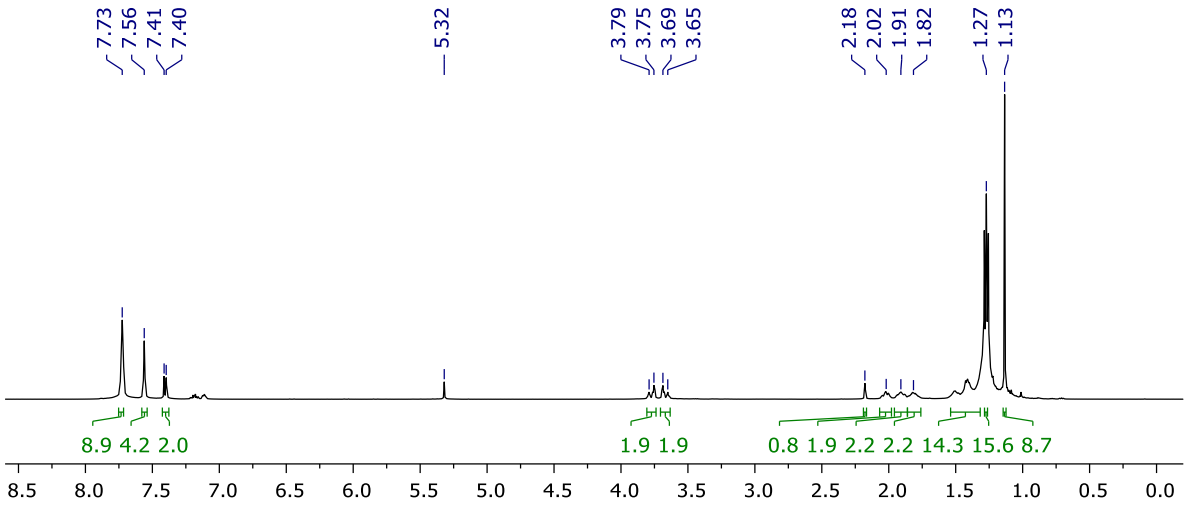

Figure S32. ^{1}H NMR spectrum of **2b** (CD_2Cl_2, 500 MHz).

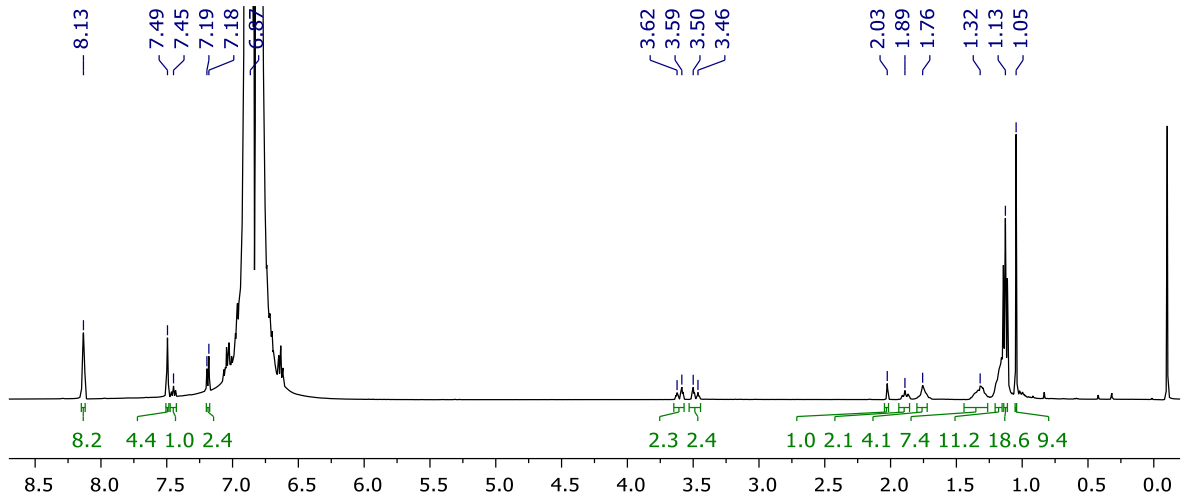

Figure S33. ^{1}H NMR spectrum of **2b** (DFB, 500 MHz).

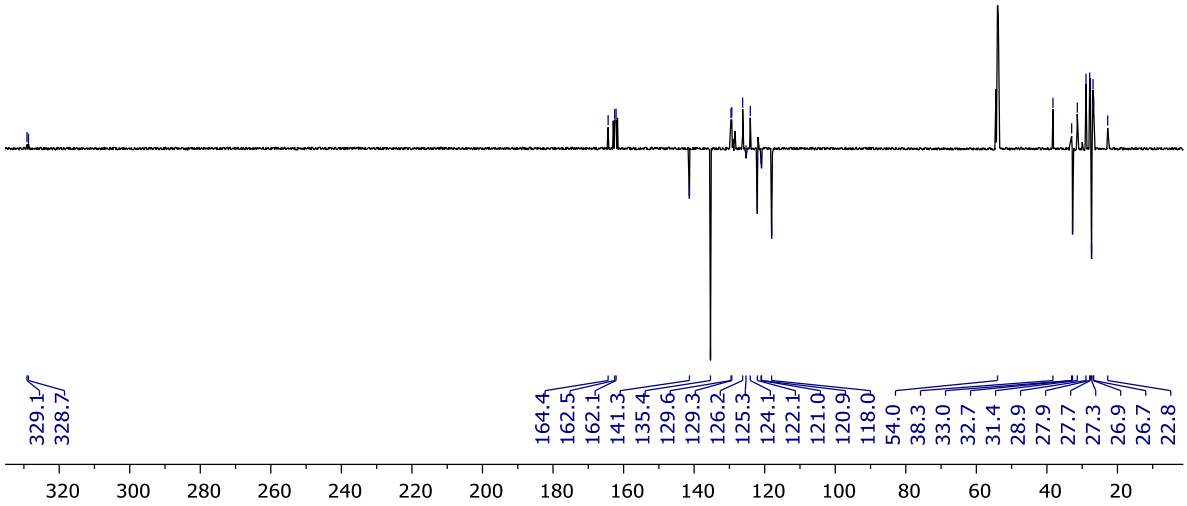

Figure S34. $^{13}C\{^{1}H\}$ APT NMR spectrum of **2b** (CD_2Cl_2, 126 MHz).

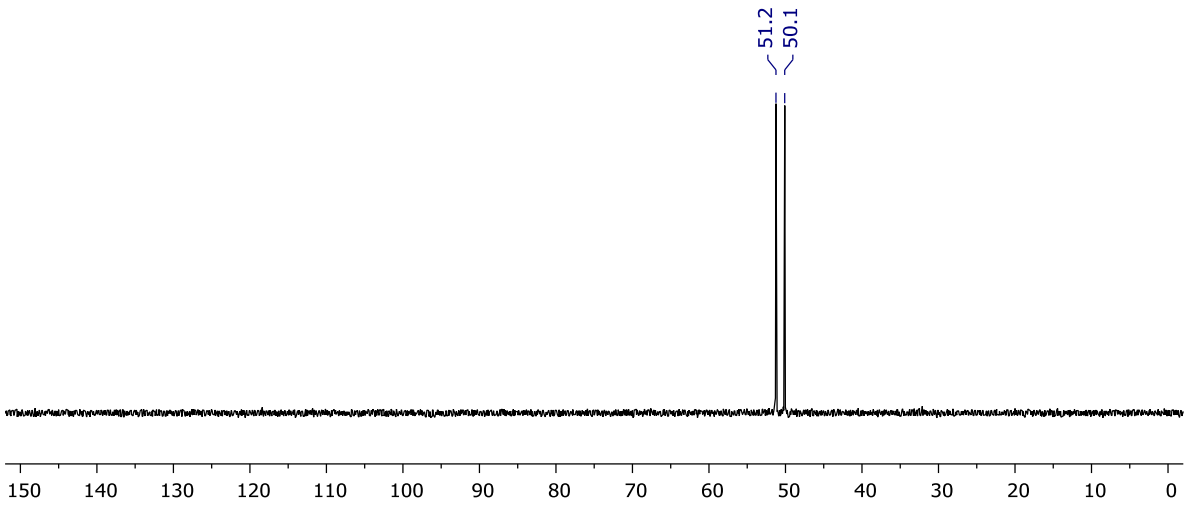

Figure S35. $^{31}P\{^{1}H\}$ NMR spectrum of **2b** (CD_2Cl_2, 121 MHz).

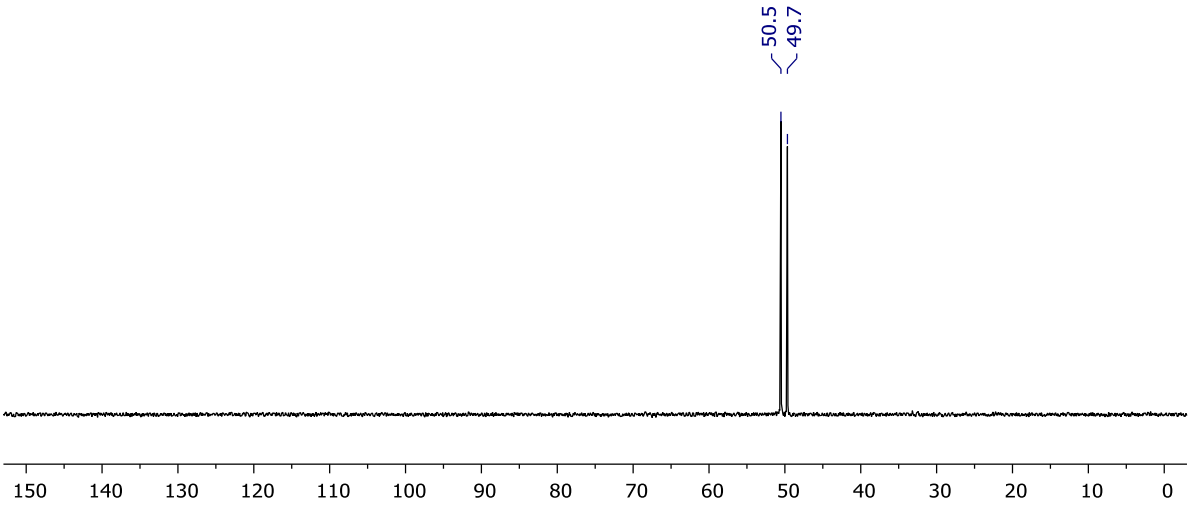

Figure S36. $^{31}P\{^{1}H\}$ NMR spectrum of **2b** (DFB, 162 MHz).

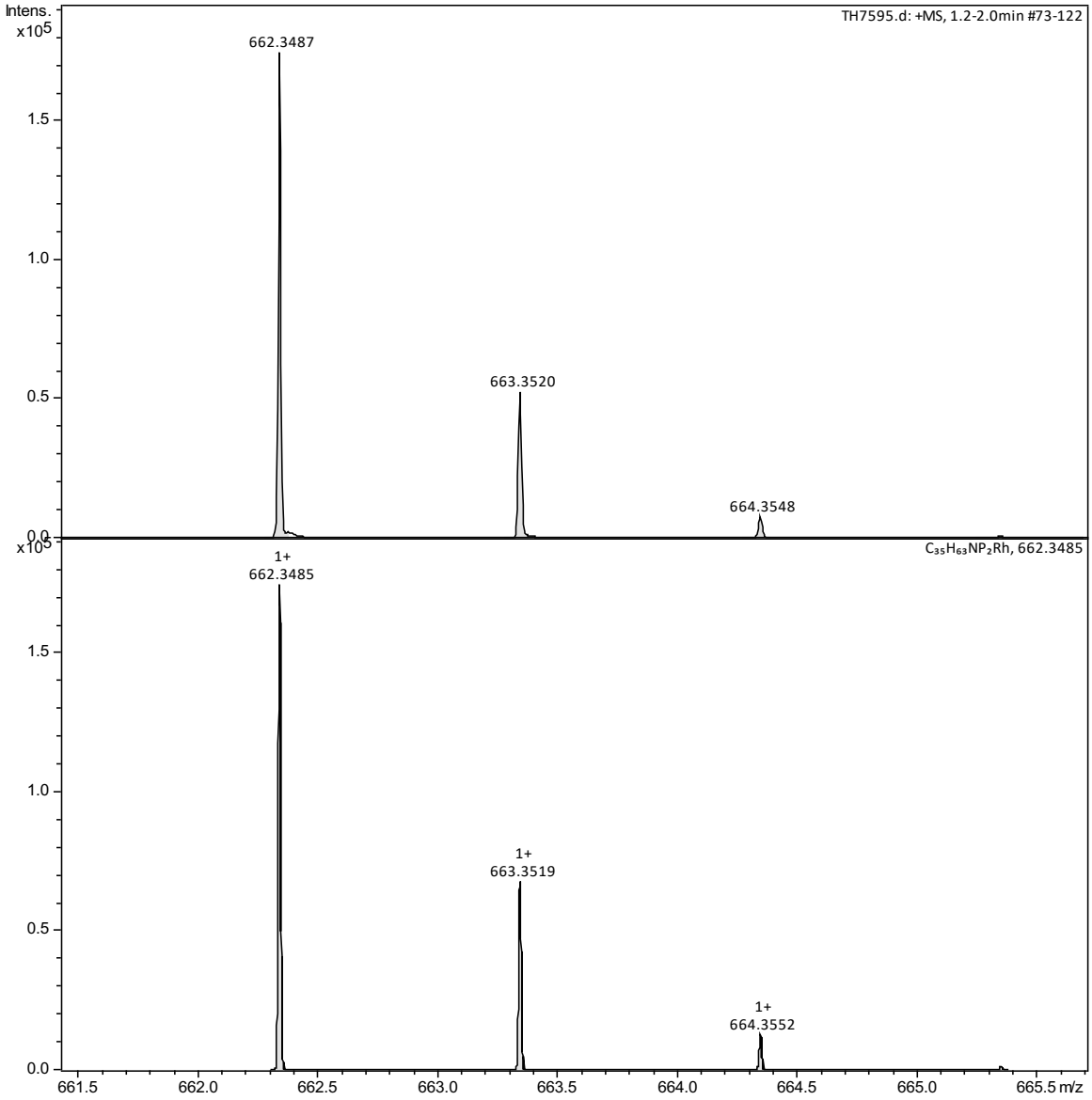

Figure S37. HR ESI-MS of **2b**.

6.3. Reaction of 2b with excess HC≡C*t*Bu

To a solution of **2b** (10.1 μmol) in DFB (0.5 mL) with excess HC≡C*t*Bu (1.5 equiv.) prepared as described above within a J. Young valve NMR tube was heated at 80 °C for 16 h. Analysis by ^{1}H and ^{31}P NMR spectroscopy indicated no reaction had occurred.

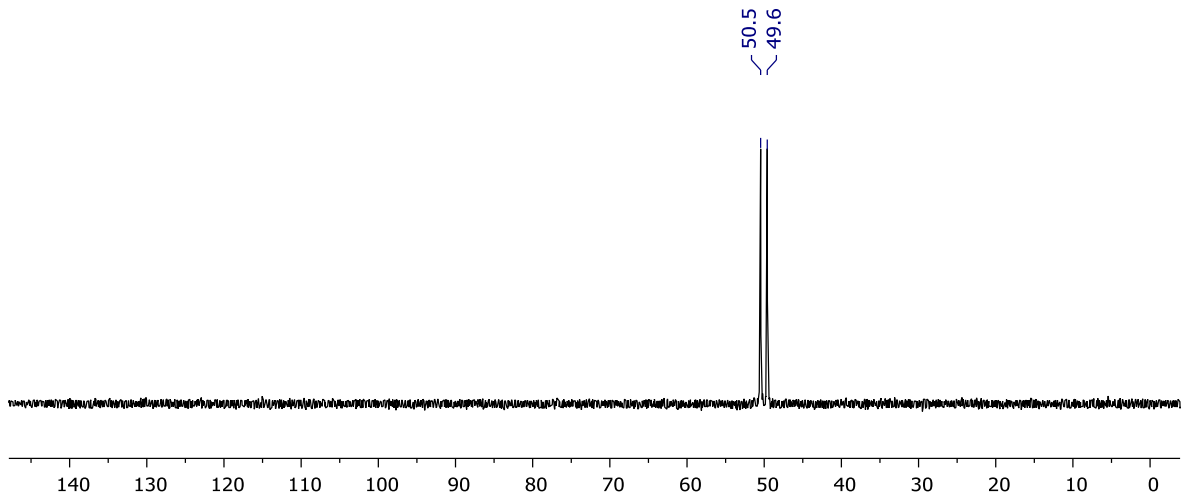

Figure S38. ^{31}P{^{1}H} NMR spectrum of the reaction between **2b** and excess HC≡C*t*Bu, after heating at 80 °C for 16 h (DFB, 162 MHz).

6.4. Reaction of 2b with excess DC≡C*t*Bu

To a solution of isolated **2b** (15.2 mg, 9.96 μmol) in DFB (355 μL) within a J. Young valve NMR tube was added DC≡C*t*Bu (12.3 μL, 98.7 μmol). The resulting solution heated was at 80 °C for 16 h. Volatiles were removed *in vacuo* and the residue analysed by ^{1}H NMR spectroscopy in CD_2Cl_2, which indicated 54% D incorporation into the vinylidene. Analysis by HR ESI-MS was uninformative.

^{1}H NMR (500 MHz, CD_2Cl_2, d_1 = 5 s, selected data): δ 2.18 (s, 0.46H, CC<u>H</u>*t*Bu).

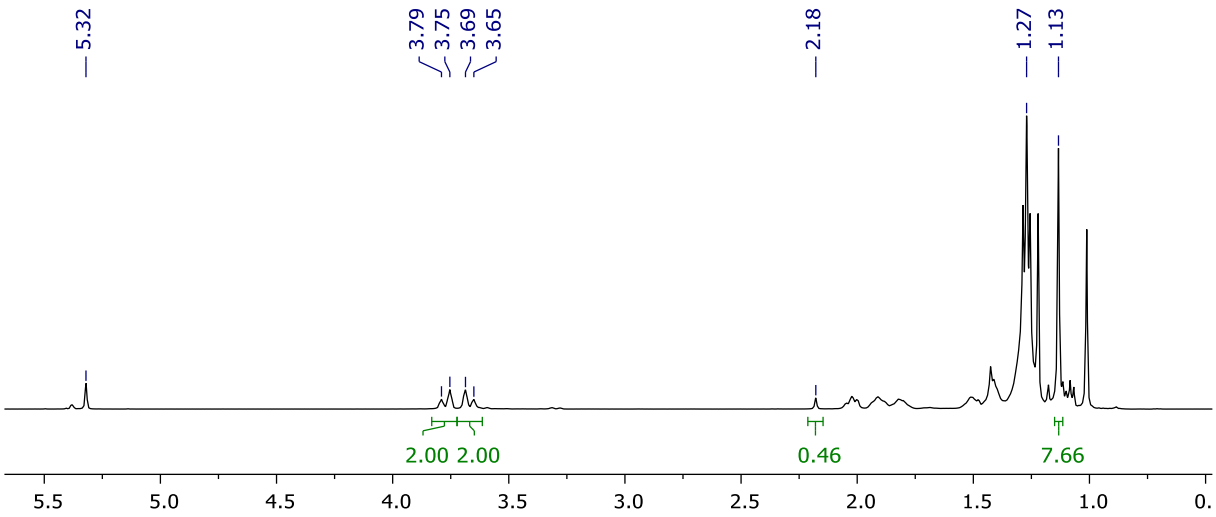

Figure S39. ^{1}H NMR spectrum of the reaction of **2b** and DC≡C*t*Bu (CD_2Cl_2, 500 MHz).

6.5. Reaction of 2b with CO

A solution of isolated **2b** (13.9 mg, 9.11 μmol) in DFB (0.50 mL) within a J. Young valve NMR tube was freeze-pump-thaw degassed and placed under an atmosphere of carbon monoxide (1 atm). Analysis by ^{1}H and ^{31}P NMR spectroscopy indicated quantitative formation of **4b** and liberation of free alkyne within 1 h, by comparison to sample of **4b** independently prepared as described below from **1b**.

^{31}P{^{1}H} NMR (162 MHz, DFB): δ 60.8 (d, $^{1}J_{RhP}$ = 122).

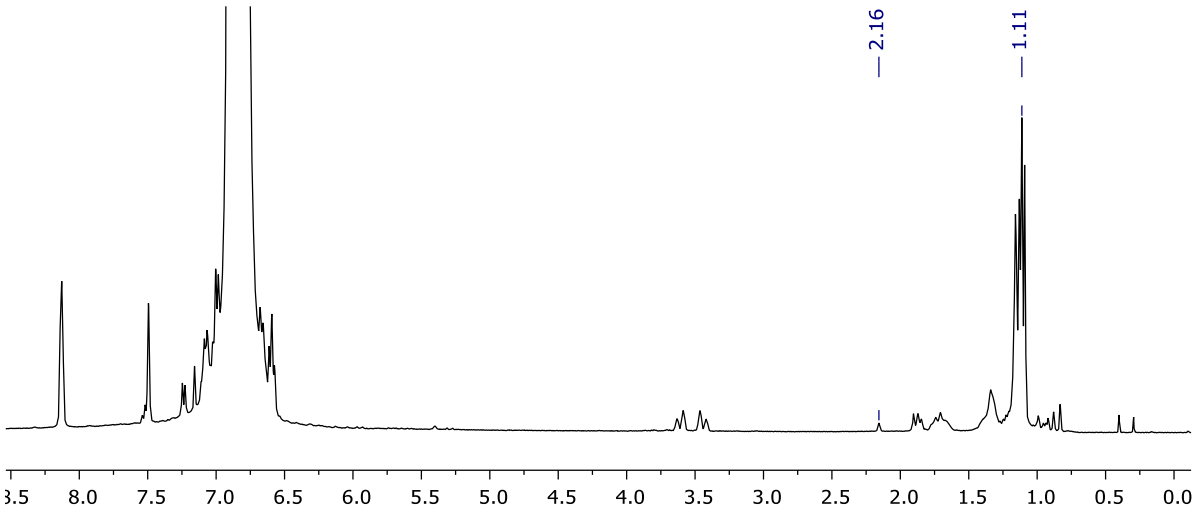

Figure S40. ^{1}H NMR spectrum of the reaction between **2b** and carbon monoxide (DFB, 400 MHz).

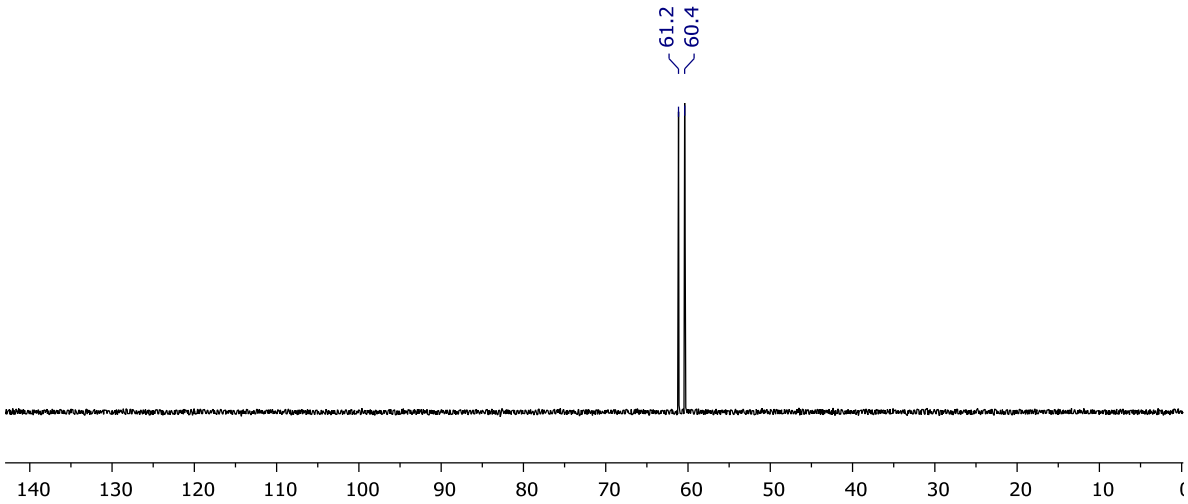

Figure S41. ^{31}P{^{1}H} NMR spectrum of the reaction between **2b** and carbon monoxide (DFB, 162 MHz).

7. Preparation of [Rh(*trans*-PNP-14)(*E*-*t*BuC≡CCHCH*t*Bu)][BAr$^F_4$] (3a)

A solution of **2a** (17.4 μmol) in DFB (0.5 mL) with excess HC≡C*t*Bu (4 equiv.) prepared as described above within a J. Young valve NMR tube was heated at 80 °C for 16 h forming a yellow solution. Volatiles were removed *in vacuo* and the resulting orange oil washed with $SiMe_4$ (0.5 mL). Recrystallisation by slow diffusion of $SiMe_4$ into an Et_2O solution at -30 ºC afforded the product was obtained as a yellow crystalline solid. Yield: 24.3 mg (15.1 μmol, 87%).

^{1}H NMR (500 MHz, CD_2Cl_2): *δ* 7.78 (t, $^3J_{HH}$ = 7.8, 1H, py), 7.70–7.74 (m, 8H, Ar^F), 7.56 (br, 4H, Ar^F), 7.41 (d, $^3J_{HH}$ = 15.6, 1H, CH=C<u>H</u>*t*Bu), 7.36 (d, $^3J_{HH}$ = 7.8, 1H, py), 7.35 (d, $^3J_{HH}$ = 7.8, 1H, py), 5.98 (d, $^3J_{HH}$ = 15.6, 1H, C<u>H</u>=CH*t*Bu), 3.36 (dd, $^2J_{HH}$ = 15.9, $^2J_{PH}$ = 4.1, 1H, py<u>CH$_2$</u>), 3.54 (dd, $^2J_{HH}$ = 15.5, $^2J_{PH}$ = 9.2, 1H, py<u>CH$_2$</u>), 3.48 (dd, $^2J_{HH}$ = 15.5, $^2J_{PH}$ = 5.7, 1H, py<u>CH$_2$</u>), 3.43 (dd, $^2J_{HH}$ = 15.9, $^2J_{PH}$ = 9.9, 1H, py<u>CH$_2$</u>), 2.15–2.28 (m, 1H, CH_2), 1.95–2.09 (m, 1H, PCH_2), 1.80–1.92 (m, 1H, PCH_2), 1.70 (s, 9H, C≡C*t*Bu), 1.05–1.77 (m, 25H, CH_2), 1.21 (s, 9H, CH=CH<u>*t*Bu</u>), 0.97 (d, $^3J_{PH}$ = 12.7, 9H, P*t*Bu), 0.84 (d, $^3J_{PH}$ = 12.7, 9H, P*t*Bu).

^{13}C{^{1}H} NMR (126 MHz, CD_2Cl_2): *δ* 163.3 (d, $^2J_{PC}$ = 5, py), 162.6 (d, $^2J_{PC}$ = 4, py), 162.3 (q, $^1J_{CB}$ = 50, Ar^F), 155.9 (s, CH=<u>C</u>H*t*Bu), 141.3 (s, py), 135.4 (s, Ar^F), 129.4 (qq, $^2J_{FC}$ = 32, $^3J_{CB}$ = 3, Ar^F), 125.2 (q, $^1J_{FC}$ = 272, Ar^F), 121.7 (d, $^3J_{PC}$ = 7, py), 121.3 (d, $^3J_{PC}$ = 7, py), 118.0 (sept, $^3J_{FC}$ = 4, Ar^F), 114.3 (s, <u>C</u>H=CH*t*Bu), 84.3 (d, $^1J_{RhC}$ = 12, C≡<u>C</u>*t*Bu), 64.8 (d, $^1J_{RhC}$ = 11, <u>C</u>≡C*t*Bu), 40.7 (dd, $^1J_{PC}$ = 17, $^3J_{PC}$ = 2, py<u>C</u>H$_2$), 39.4 (dd, $^1J_{PC}$ = 17, $^3J_{PC}$ = 2, py<u>C</u>H$_2$), 35.3 (s, CH=CH<u>*t*Bu</u>{C}), 34.1 (s, C≡C<u>*t*Bu</u>{C}), 33.8 (vt, J_{PC} = 8, P*t*Bu{C}), 33.6 (br d, $^1J_{PC}$ = 13, P*t*Bu{C}), 32.6 (s, C≡C<u>*t*Bu</u>{CH$_3$}), 31.6 (d, J_{PC} = 10, CH_2), 31.0 (s, CH_2), 30.9 (s, CH_2), 30.8 (d, J_{PC} = 6, CH_2), 30.52 (s, CH_2), 30.49 (s, CH_2), 30.4 (s, CH=CH<u>*t*Bu</u>{CH$_3$}), 30.3 (s, CH_2), 29.8 (s, CH_2), 29.5 (s, CH_2), 29.1 (s, CH_2), 29.0 (d, $^2J_{PC}$ = 5, P*t*Bu{CH$_3$}), 28.7 (d, $^2J_{PC}$ = 5, P*t*Bu{CH$_3$}), 27.1–27.4 (m, PCH_2), 26.5 (d, J_{PC} = 4, CH_2), 25.9 (d, J_{PC} = 2, CH_2), 25.6–25.8 (m, PCH_2).

^{31}P{^{1}H} NMR (162 MHz, CD_2Cl_2): *δ* 57.6 (dd, $^2J_{PP}$ = 392, $^1J_{RhP}$ = 133, 1P), 51.9 (dd, $^2J_{PP}$ = 392, $^1J_{RhP}$ = 129, 1P).

HR ESI-MS (positive ion 4 kV): 744.4263, ([*M*]$^+$, calcd 744.4268) *m/z*.

Anal. Calcd for $C_{73}H_{85}BF_{24}NP_2Rh$ (1608.11 gmol^{-1}): C, 54.52; H, 5.33; N, 0.87. Found: C, 54.38; H, 5.41; N, 0.88.

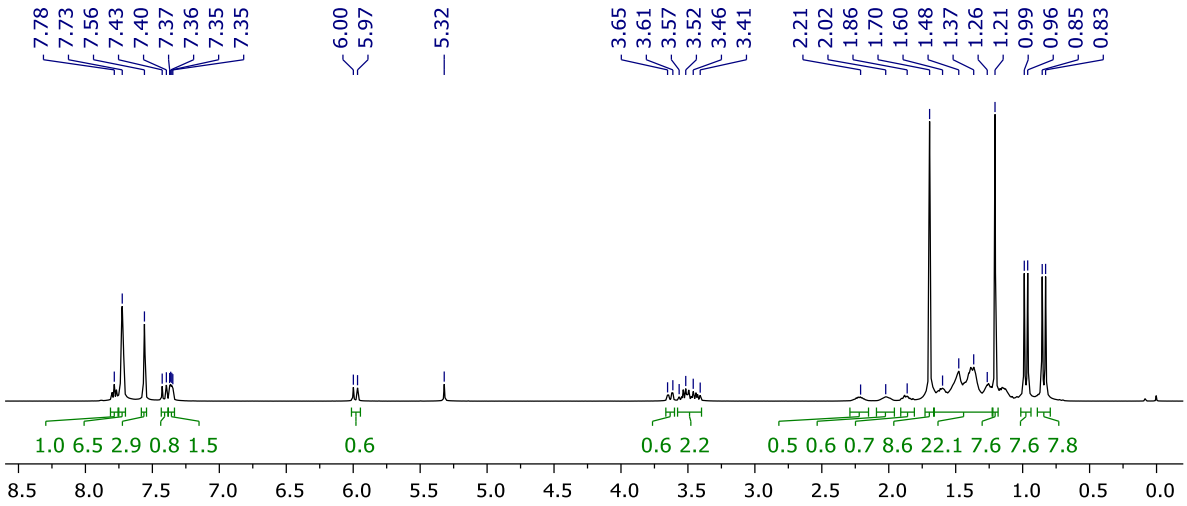

Figure S42. ^{1}H NMR spectrum of **3a** (CD_2Cl_2, 500 MHz).

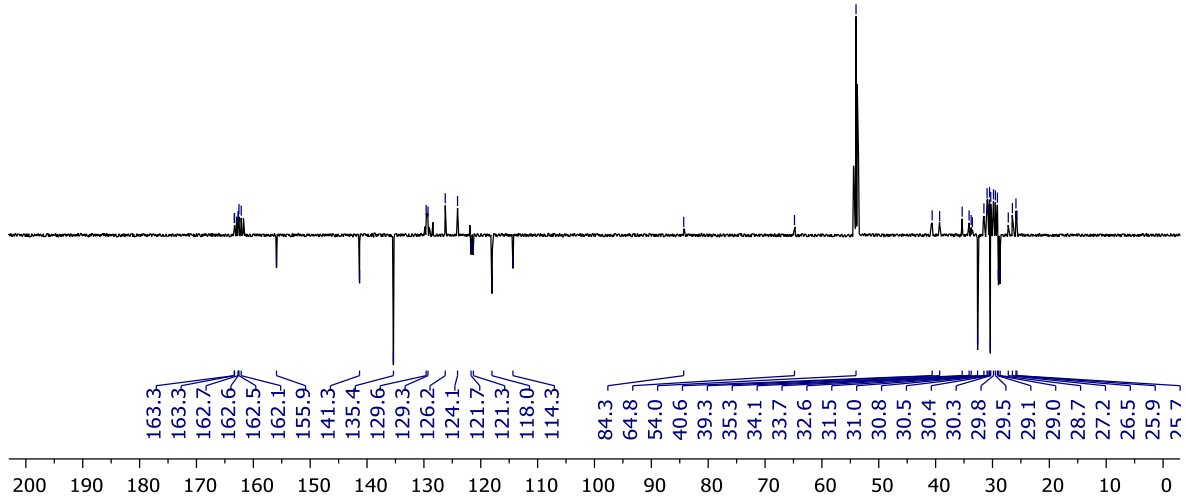

Figure S43. $^{13}C\{^{1}H\}$ APT NMR spectrum of **3a** (CD_2Cl_2, 126 MHz).

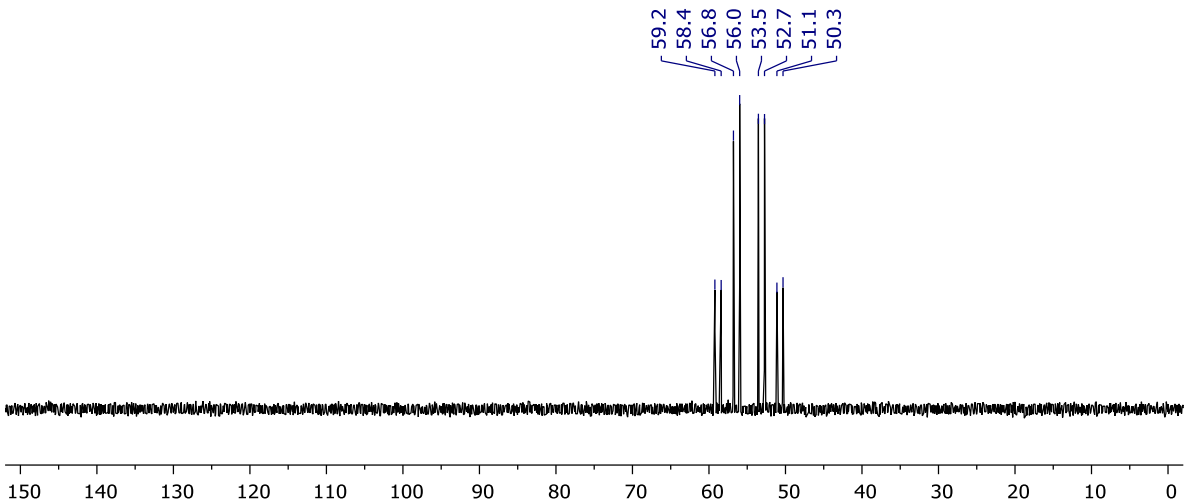

Figure S44. $^{31}P\{^{1}H\}$ NMR spectrum of **3a** (CD_2Cl_2, 162 MHz).

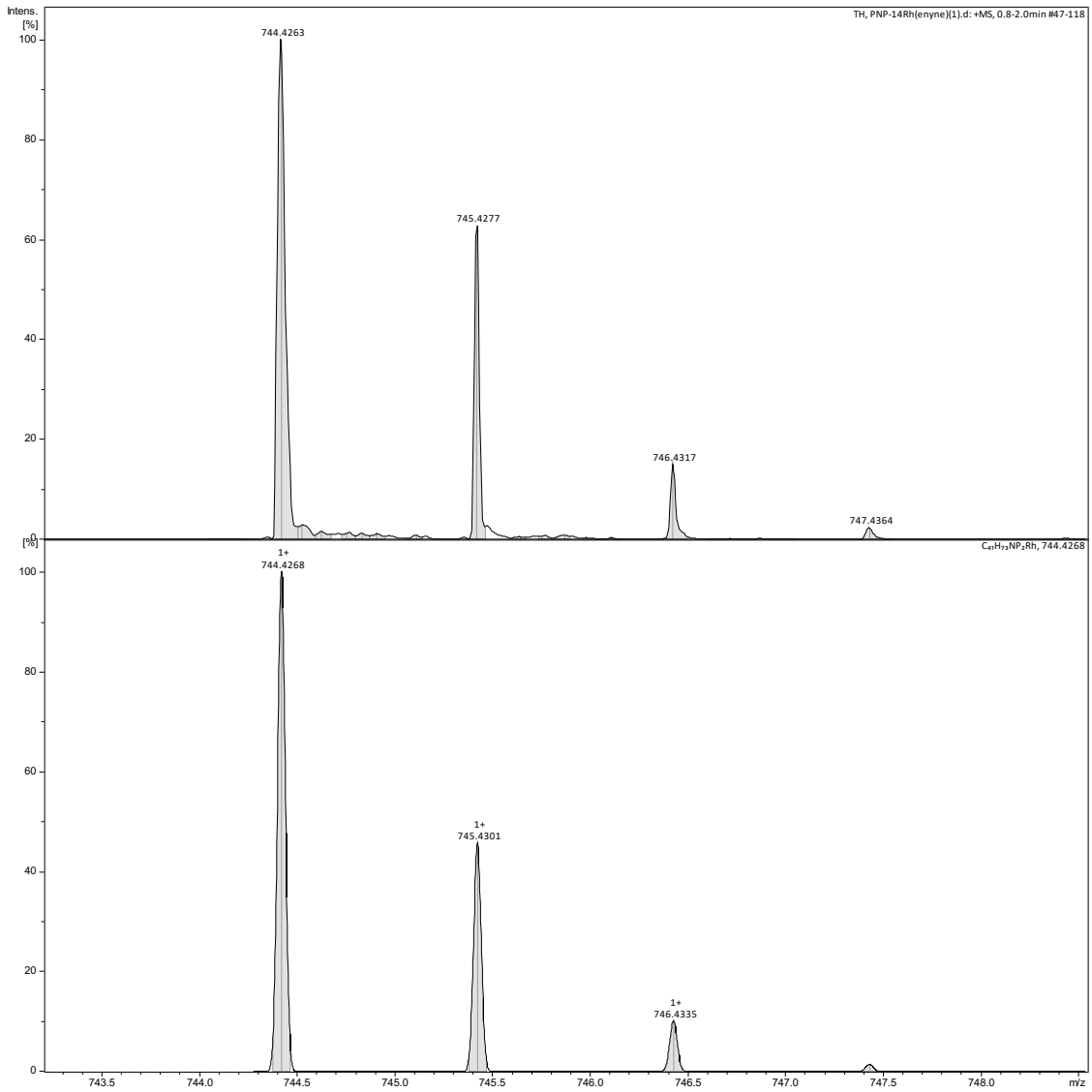

Figure S45. HR ESI-MS of **3a**.

8. Reaction of {Rh(*trans*-PNP-14)}$^+$ (1a) with *E*-*t*BuC≡CCHCH*t*Bu

A solution of *trans*-PNP-14 (5.8 mg, 12.1 μmol) and [Rh(COD)$_2$][BAr$^F{}_4$] (14.3 mg, 12.1 μmol) in DFB (0.5 mL) within a J. Young valve NMR tube was mixed for 5 min at RT and *E*-*t*BuC≡CCHCH*t*Bu (12.5 mg, 76.1 μmol) added. The resulting solution was stirred for 1 h at RT and volatiles removed *in vacuo*. The resulting orange oil was washed with $SiMe_4$ (3×0.5 mL) and dried to afford the non-interpenetrated enyne isomer of **3a** [Rh(*trans*-PNP-14)(exo-*E*-*t*BuC≡CCHCH*t*Bu)][BAr$^F{}_4$] (**3a′**) as the exclusive organometallic product as an orange foam, which was characterised *in situ* and carried forward without further purification.

^{1}H NMR (500 MHz, DFB, selected data): *δ* 7.48 (t, $^3J_{HH}$ = 7.8, 1H, py), 7.14–7.18 (m, 2H, py), 6.07 (d, $^3J_{HH}$ = 15.8, 1H, CH=C<u>H</u>*t*Bu), 5.71 (d, $^3J_{HH}$ = 15.8, 1H, C<u>H</u>=CH*t*Bu), 3.47 (dd, $^2J_{HH}$ = 17.4, $^2J_{PH}$ = 5.4, 1H, pyC<u>H</u>$_2$), 3.39 (ddd, $^2J_{HH}$ = 17.4, $^2J_{PH}$ = 10.7, $^4J_{PH}$ = 3.4, 1H, pyC<u>H</u>$_2$), 3.26 (br dd, $^2J_{HH}$ = 17.8,

$^{2}J_{PH}$ = 10.4, 1H, pyC<u>H</u>$_2$), 3.12 (dd, $^{2}J_{HH}$ = 17.8, $^{2}J_{PH}$ = 8.4, 1H, pyC<u>H</u>$_2$), 1.34 (s, 9H, C≡C<u>*t*Bu</u>), 1.04 (s, 9H, CH=CH<u>*t*Bu</u>), 0.88 (d, $^{3}J_{PH}$ = 12.8, 9H, P*t*Bu), 0.87 (d, $^{3}J_{PH}$ = 13.9, 9H, P*t*Bu).

^{13}C{^{1}H} NMR (126 MHz, DFB, selected data): *δ* 164.2 (dd, $^{2}J_{PC}$ = 8, J_{PC} = 3, py), 161.4 (d, $^{2}J_{PC}$ = 6, py), 153.5 (s, CH=<u>C</u>H*t*Bu), 139.0 (s, py), 121.1 (d, $^{3}J_{PC}$ = 9, py), 120.6 (d, $^{3}J_{PC}$ = 9, py), 110.4 (s, <u>C</u>H=CH*t*Bu), 88.0 (d, $^{1}J_{RhC}$ = 18, C≡<u>C</u>*t*Bu), 67.8 (dd, $^{1}J_{RhC}$ = 9, $^{2}J_{PC}$ = 4, <u>C</u>≡C*t*Bu), 38.8 (br d, $^{1}J_{PC}$ = 18, py<u>C</u>H$_2$), 36.5 (br d, $^{1}J_{PC}$ = 16, py<u>C</u>H$_2$), 31.0 (s, C≡C<u>*t*Bu</u>{CH$_3$}), 28.9 (s, CH=CH<u>*t*Bu</u>{CH$_3$}), 28.5 (d, $^{2}J_{PC}$ = 4, P*t*Bu{CH$_3$}), 25.1 (d, $^{2}J_{PC}$ = 5, P*t*Bu{CH$_3$}).

^{31}P{^{1}H} NMR (162 MHz, DFB): *δ* 44.3 (dd, $^{2}J_{PP}$ = 408, $^{1}J_{RhP}$ = 131, 1P), 36.9 (dd, $^{2}J_{PP}$ = 408, $^{1}J_{RhP}$ = 128, 1P).

HR ESI-MS (positive ion 4 kV): 774.4383 ([*M*]$^{+}$, calcd 744.4286) *m/z*.

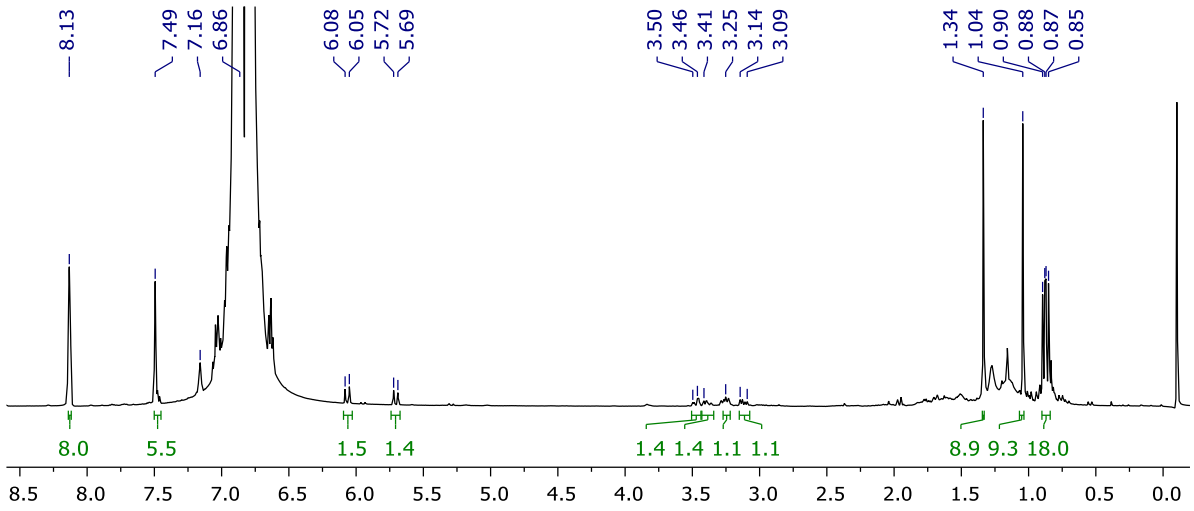

Figure S46. ^{1}H NMR spectrum of **3a′** (DFB, 500 MHz).

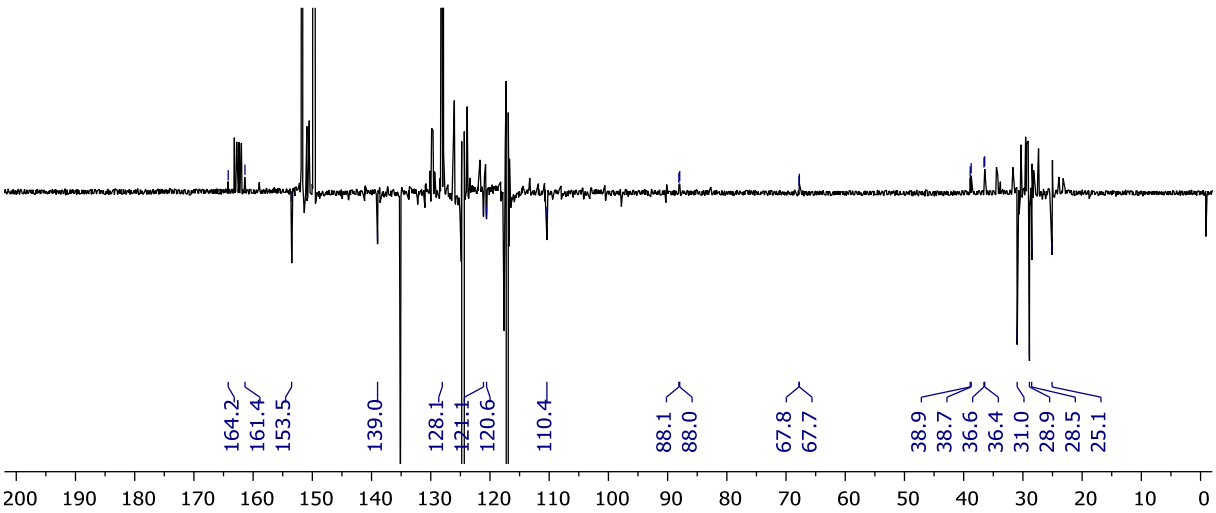

Figure S47. ^{13}C{^{1}H} APT NMR spectrum of **3a′** (DFB, 126 MHz).

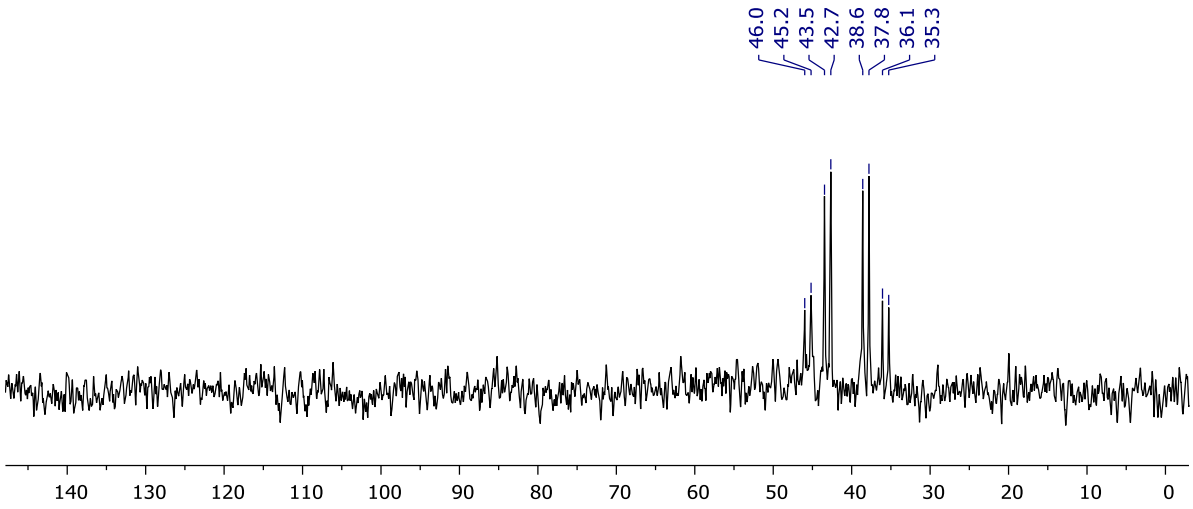

Figure S48. $^{31}P\{^{1}H\}$ NMR spectrum of **3a′** (DFB, 162 MHz).

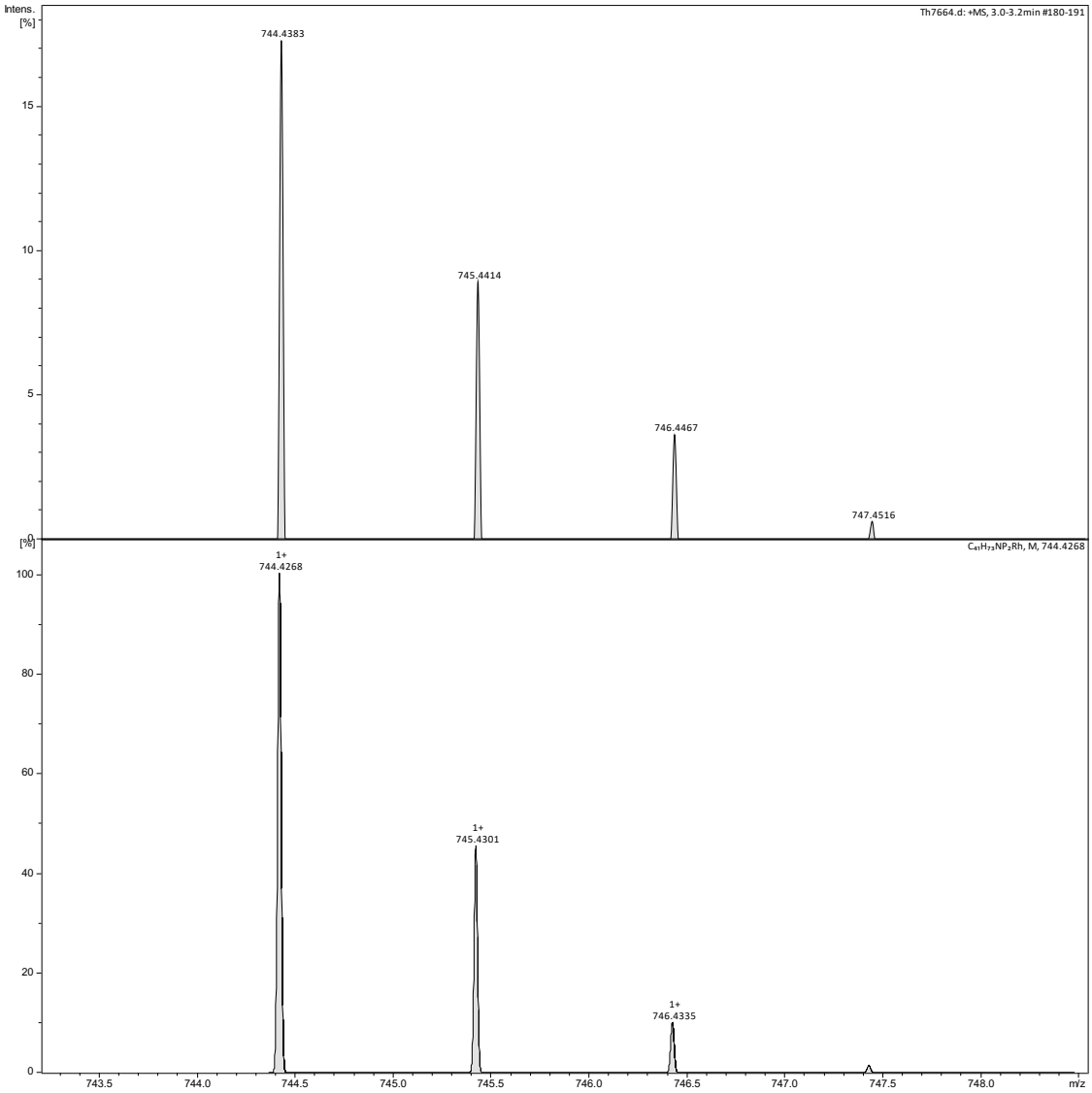

Figure S49. ESI-MS of **3a′**.

A solution of **3a′** (12.1 μmol) in DFB (0.5 mL) within a J. Young valve NMR tube was heated at 80 °C for 5 days. Analysis by ^{1}H and ^{31}P NMR spectroscopy indicated complete consumption of **3a′**, formation of a derivative where the ring has been dehydrogenated, [Rh(*trans*-PNP-14′)][BAr$^{F}_{4}$] (**5a**), as the major organometallic product (>80%) alongside *E*,*E*-*t*BuCH=CHCH=CH*t*Bu (*δ* 5.87 (2H), 5.50 (2H), 0.92 (18H))[6] from transfer hydrogenation of *E*-*t*BuC≡CCHCH*t*Bu. Volatiles were removed *in vacuo* and the residue extracted with hot heptane to afford the product, which was characterised *in situ*. Based on this data we cannot discriminate between formulations featuring an internal *E*- or *Z*-alkene, and it is possible the balance of the material is the alternative isomer. Indeed, a handful of single crystals were obtained by recrystallisation from heptane and analysis by X-ray diffraction indicated a mixture of *E*- and *Z*-alkene isomers. We do not think this is representative of the bulk, but nevertheless this solution further corroborates dehydrogenation of the methylene chain.

^{1}H NMR (500 MHz, CD_2Cl_2, selected data): *δ* 7.73 (obscured, 1H, py), 7.36 (d, $^{3}J_{HH}$ = 7.8, 1H, py), 7.29 (d, $^{3}J_{HH}$ = 7.8, 1H, py), 5.13–5.21 (m, 1H, CH=CH), 4.31–4.40 (m, 1H, CH=CH), 3.60–3.75 (m, 3H, 3×pyC$\underline{H}_2$), 3.34–3.43 (m, 1H, pyC$\underline{H}_2$), 1.04 (d, $^{3}J_{PH}$ = 14.6, 9H, *t*Bu), 0.84 (d, $^{3}J_{PH}$ = 13.9, 9H, *t*Bu).

^{13}C{^{1}H} NMR (126 MHz, CD_2Cl_2, selected data): *δ* 130.8 (s, py), 121.7 (overlapping d, $^{3}J_{PC}$ = 9, 2×py), 88.3 (dd, $^{1}J_{RhC}$ = 11, $^{2}J_{PC}$ = 4, CH=CH) 70.3 (d, $^{1}J_{RhC}$ = 8, CH=CH), 39.5 (d, $^{1}J_{PC}$ = 18, py$\underline{C}H_2$), 36.8 (br d, $^{1}J_{PC}$ = 15, py$\underline{C}H_2$), 26.9 (d, $^{2}J_{PC}$ = 4, P*t*Bu{CH_3}), 26.7 (d, $^{2}J_{PC}$ = 5, P*t*Bu{CH_3}).

^{31}P{^{1}H} NMR (162 MHz, CD_2Cl_2): *δ* 89.7 (dd, $^{2}J_{PP}$ = 301, $^{1}J_{RhP}$ = 128, 1P), 53.0 (dd, $^{2}J_{PP}$ = 301, $^{1}J_{RhP}$ = 124, 1P).

^{31}P{^{1}H} NMR (162 MHz, DFB): *δ* 90.0 (dd, $^{2}J_{PP}$ = 300, $^{1}J_{RhP}$ = 128, 1P), 52.4 (dd, $^{2}J_{PP}$ = 300, $^{1}J_{RhP}$ = 124, 1P).

HR ESI-MS (positive ion 4 kV): 578.2534 ([*M*]$^{+}$, calcd 578.2546) *m/z*.

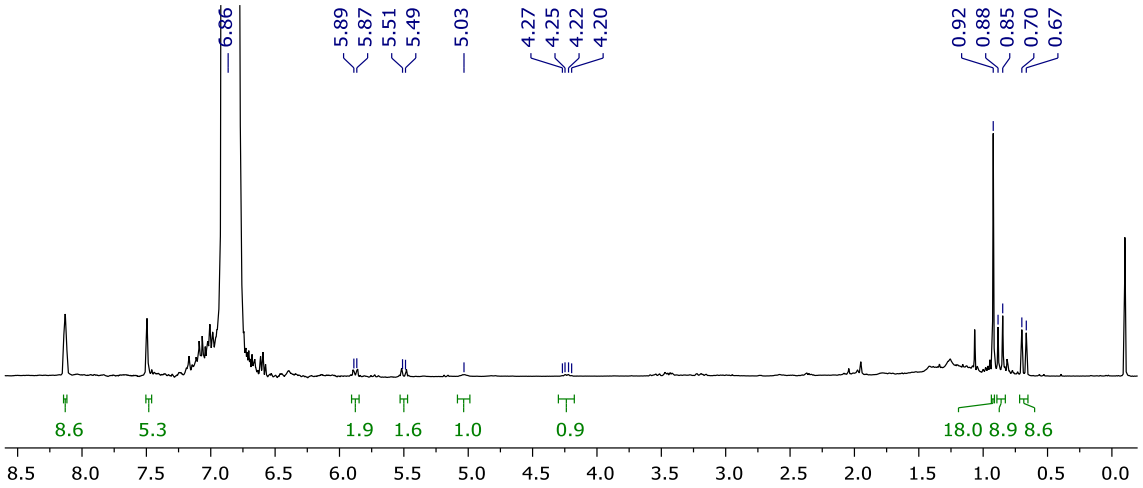

Figure S50. ^{1}H NMR spectrum collected after heating **3a′** at 80 °C for 5 days (DFB, 400 MHz).

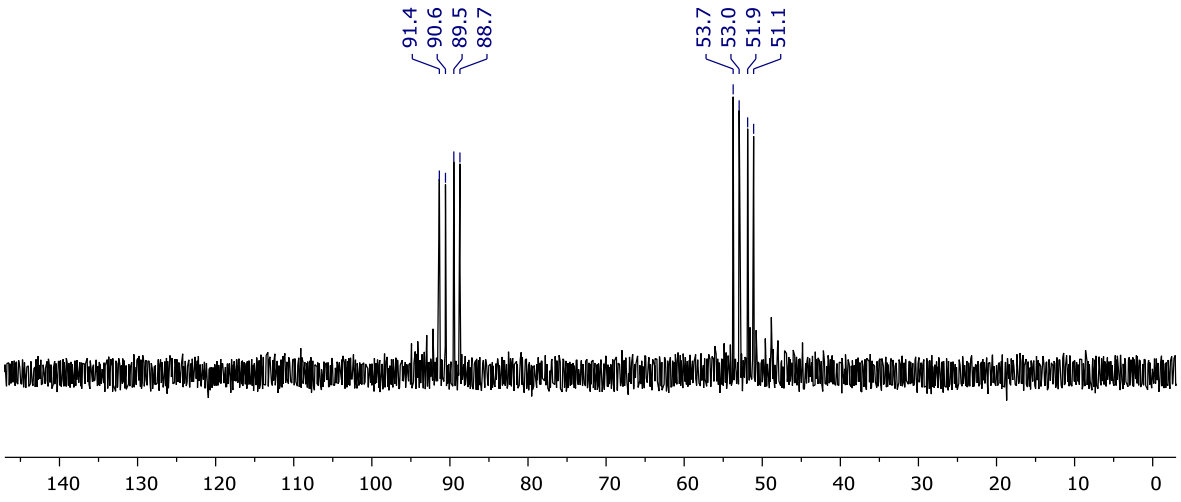

Figure S51. $^{31}P\{^{1}H\}$ NMR spectrum collected after heating **3a'** at 80 °C for 5 days (DFB, 162 MHz).

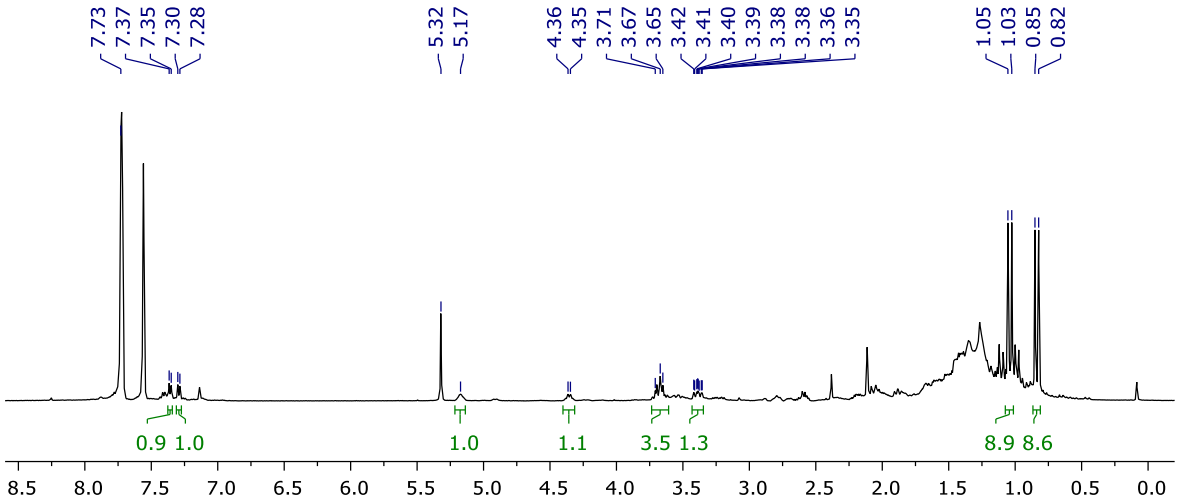

Figure S52. ^{1}H NMR spectrum of **5a** (CD_2Cl_2, 500 MHz).

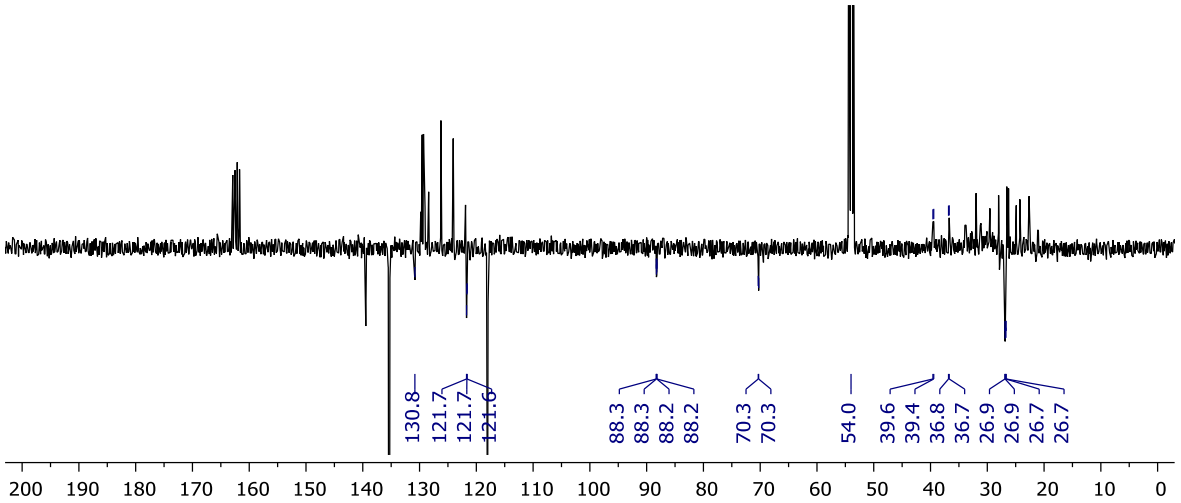

Figure S53. $^{13}C\{^{1}H\}$ APT NMR spectrum of **5a** (CD_2Cl_2, 126 MHz).

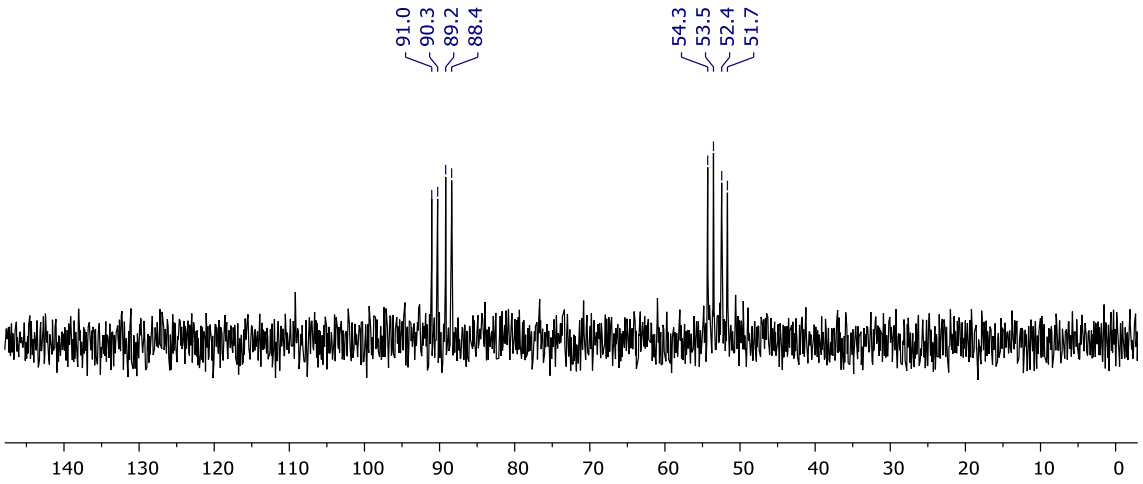

Figure S54. $^{31}P\{^{1}H\}$ NMR spectrum of **5a** (CD_2Cl_2, 162 MHz).

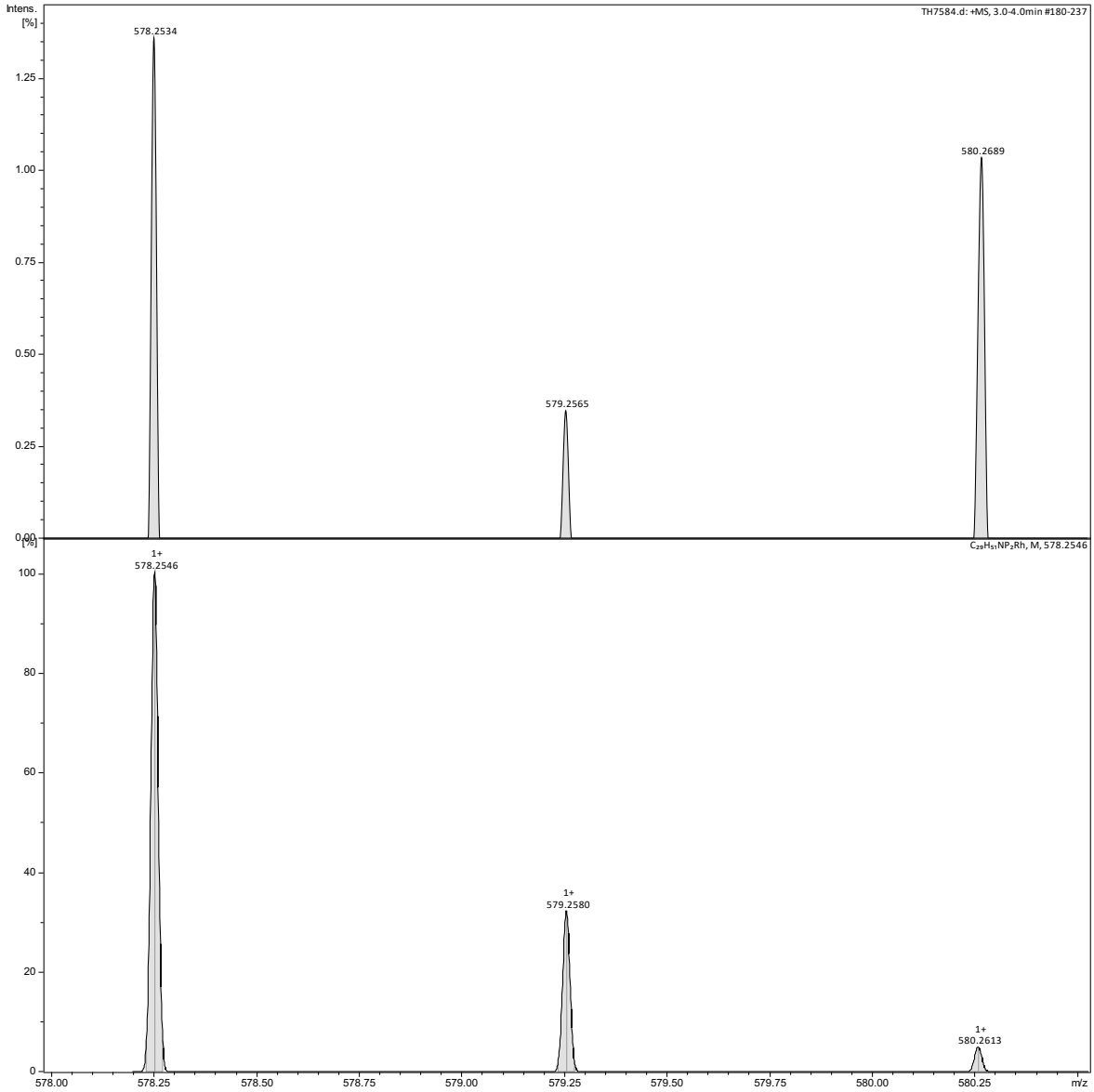

Figure S55. HR ESI-MS of **5a**.

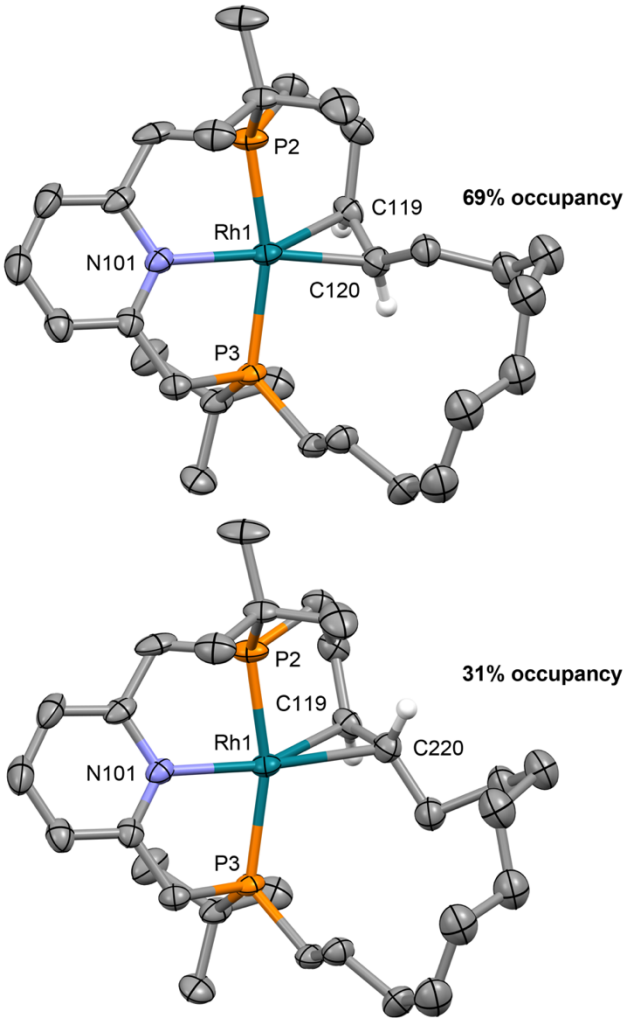

Figure S56. Solid-state structure of **5a** (both disordered components): thermal ellipsoids drawn at 30% probability, anion, solvent and most hydrogen atoms omitted. Selected bond lengths (Å) and angles (deg): Rh1-P2, 2.2349(15); Rh1-P3, 2.3153(14); Rh1-N101, 2.085(5); P2-Rh1-P3, 164.51(7); Rh1-Cnt(C119,C120), 2.038(5), Rh1-Cnt(C119,C220), 2.152(12); C119-C120 [restrained with C119-C220], 1.320(11); C119-C220, 1.336(14) [restrained with C119-C120]; N101-Rh1-Cnt(C119,C120), 167.4(2); N101-Rh1-Cnt(C119,C220), 166.4(3); Cnt = centroid.

9. Preparation of [Rh(*cis*-PNP-14)(CO)][BAr$^F_4$] (4b)

A solution of *cis*-PNP-14 (8.3 mg, 17.4 µmol) and [Rh(COD)$_2$][BAr$^F_4$] (20.6 mg, 17.4 µmol) in DFB (0.5 mL) was mixed for 5 min at RT and then freeze-pump-thaw degassed and placed under an atmosphere of carbon monoxide for 5 min. Volitates were removed to afford the product as a yellow solid after washing with SiMe$_4$ (2×0.5 mL). Yield: 20.2 mg (13.7 µmol, 79%).

^{1}H NMR (500 MHz, CD_2Cl_2): δ 7.78 (t, $^3J_{HH}$ = 7.8, 1H, py), 7.70–7.74 (m, 8H, Ar^F), 7.56 (br, 4H, Ar^F), 7.43 (d, $^3J_{HH}$ = 7.8, 2H, py), 3.75 (dvt, $^2J_{HH}$ = 18.1, J_{PH} = 4.2, 2H, pyC$\underline{H}_2$), 3.61 (dvt, $^2J_{HH}$ = 18.1, J_{PH} = 4.4, 2H, pyC$\underline{H}_2$), 1.96–2.07 (m, 2H, PCH$_2$), 1.83–1.95 (m, 2H, PCH$_2$), 1.66–1.77 (m, 2H, CH$_2$), 1.38–1.53 (m, 6H, CH$_2$), 1.22–1.38 (m, 16H, CH$_2$), 1.26 (vt, J_{PH} = 8, 18H, *t*Bu).
^{13}C{^{1}H} NMR (126 MHz, CD_2Cl_2): δ 193.6 (dt, $^1J_{RhC}$ = 69, $^2J_{PC}$ = 14, CO), 164.5 (vtd, J_{PC} = 6, $^2J_{RhC}$ = 1, py), 162.3 (q, $^1J_{CB}$ = 50, Ar^F), 141.1 (s, py), 135.4 (s, Ar^F), 129.4 (qq, $^2J_{FC}$ = 32, $^3J_{CB}$ = 3, Ar^F), 125.1 (q, $^1J_{FC}$ = 272, Ar^F), 122.5 (vt, J_{PC} = 6, py), 118.0 (sept, $^3J_{FC}$ = 4, Ar^F), 38.2 (vt, J_{PC} = 9, py$\underline{C}H_2$), 32.6 (vtd, J_{PC} = 14, $^2J_{RhC}$ = 2, *t*Bu{C}), 31.2 (vt, J_{PC} = 7, CH$_2$), 28.5 (s, CH$_2$), 27.6 (s, CH$_2$), 27.4 (s, CH$_2$) 27.1 (vt, J_{PC} = 3, *t*Bu{CH$_3$}), 27.0 (s, CH$_2$), 26.7 (s, CH$_2$), 23.9 (vtd, J_{PC} = 12, $^2J_{RhC}$ = 2, PCH$_2$).
^{31}P{^{1}H} NMR (162 MHz, CD_2Cl_2): δ 60.8 (d, $^1J_{RhP}$ = 122).
IR (CH_2Cl_2): ν(CO) 1997 cm^{-1}.
HR ESI-MS (positive ion, 4 kV): 608.2649, ([*M*]$^+$, calcd 608.2652) *m/z*.

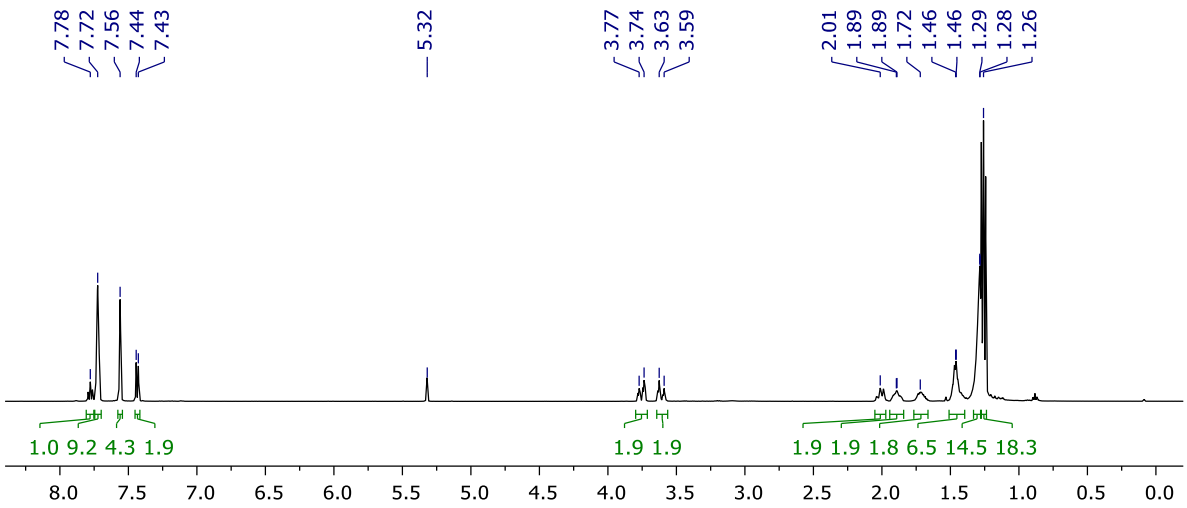

Figure S57. ^{1}H NMR spectrum of **4b** (CD_2Cl_2, 500 MHz).

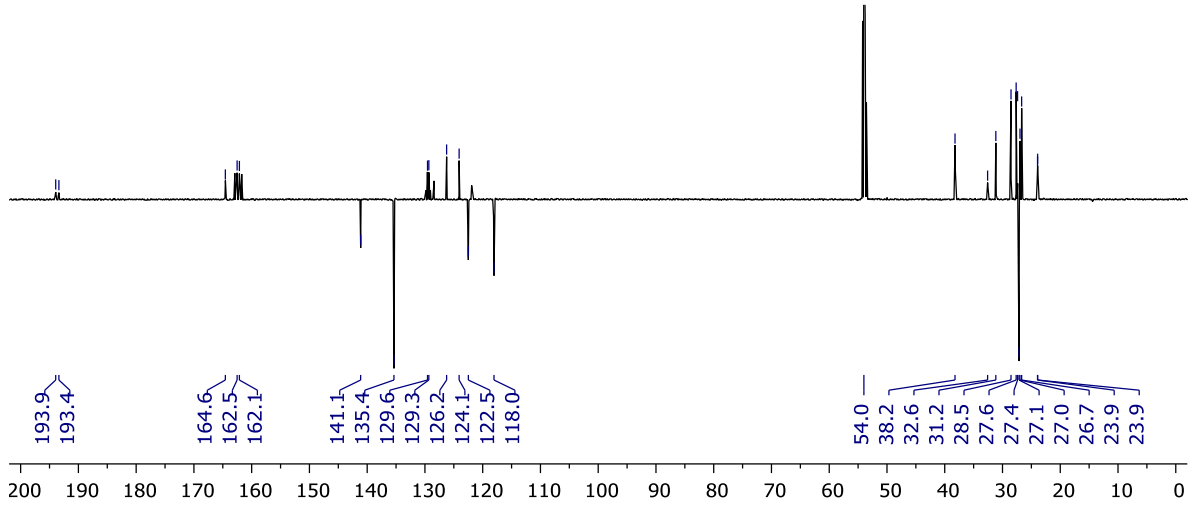

Figure S58. $^{13}C\{^{1}H\}$ APT NMR spectrum of **4b** (CD_2Cl_2, 126 MHz).

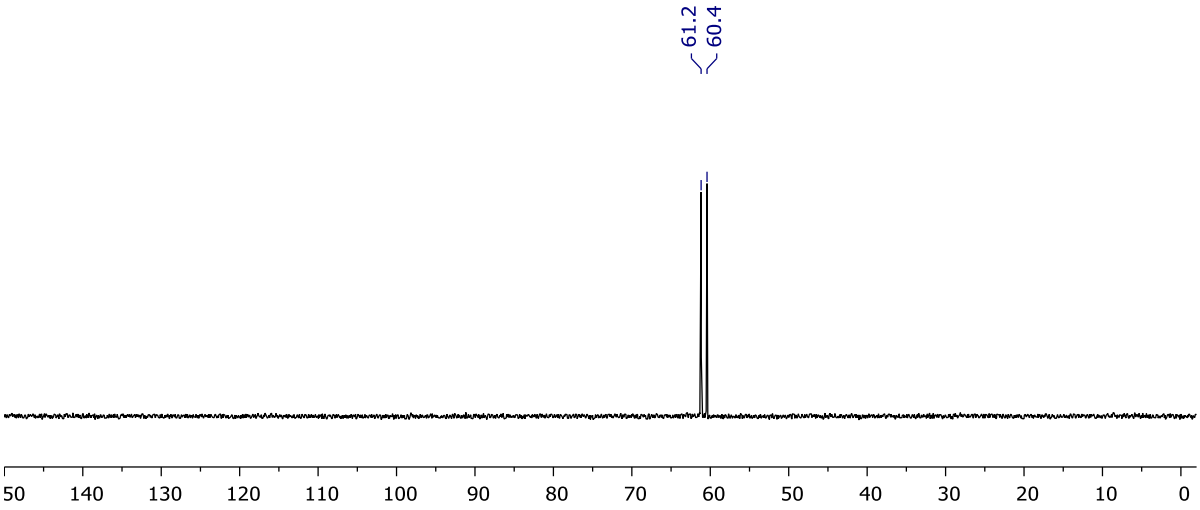

Figure S59. $^{31}P\{^{1}H\}$ APT NMR spectrum of **4b** (CD_2Cl_2, 162 MHz).

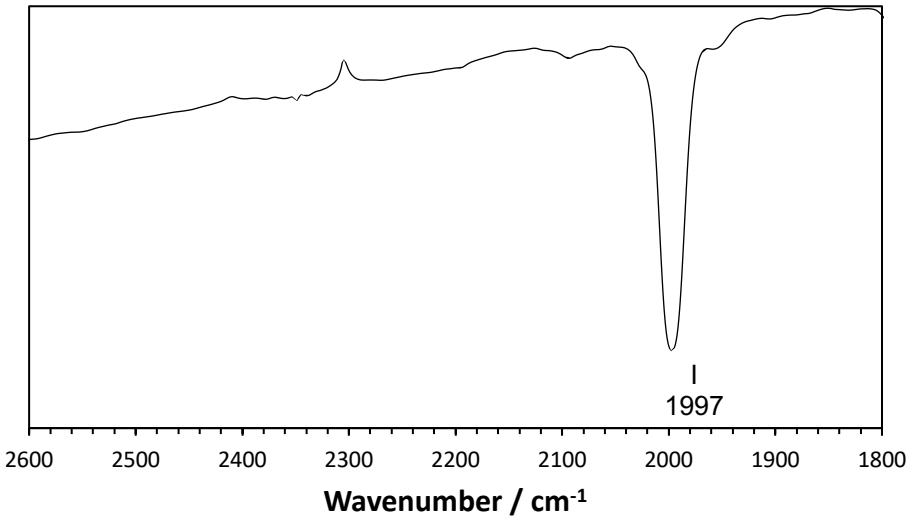

Figure S60. IR spectrum of **4b** recorded in CH_2Cl_2.

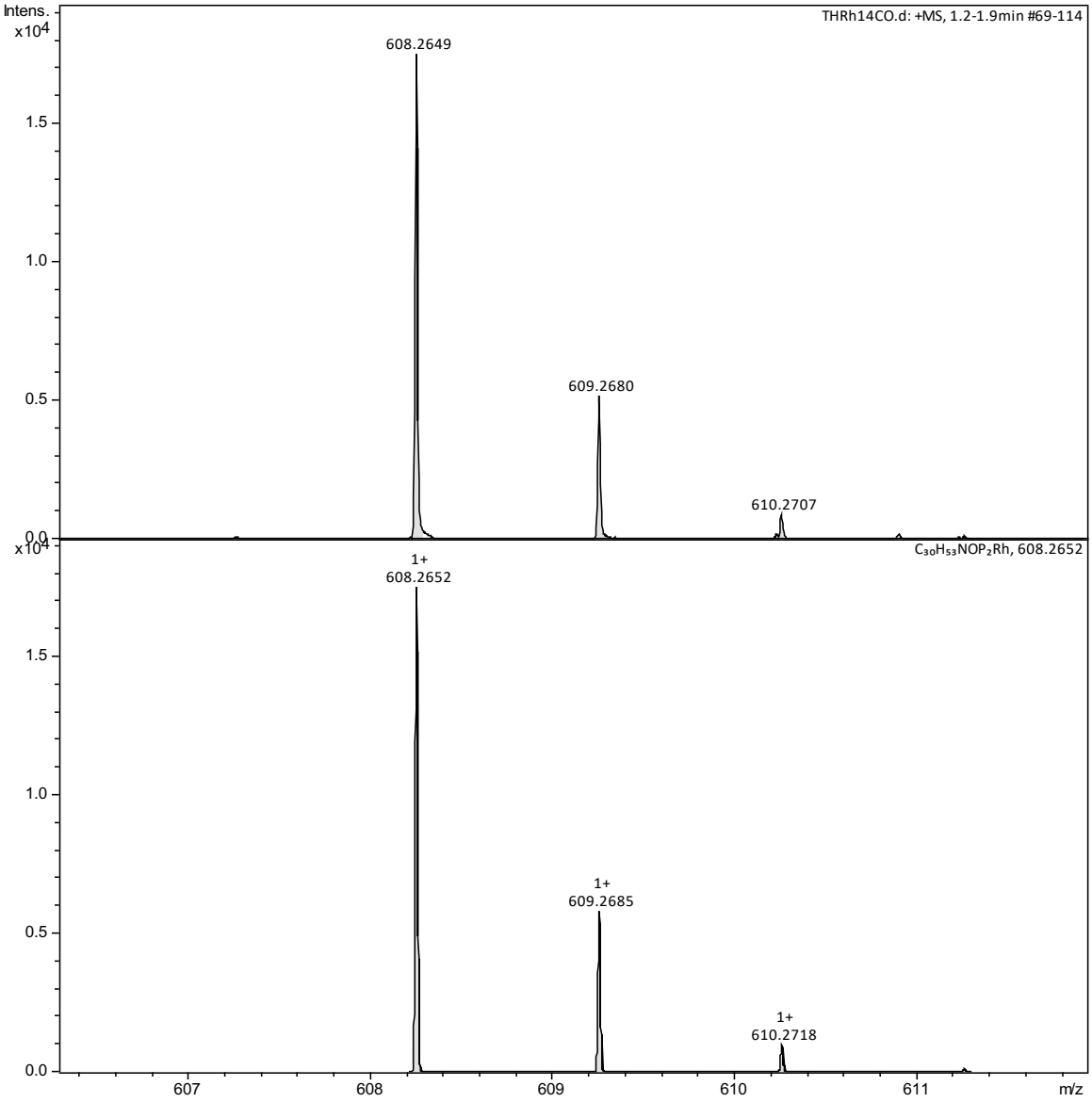

Figure S61. HR ESI-MS of **4b**.

10. Preparation of [Rh(*trans*-PONOP-14)(*E*-*t*BuC≡CCHCH*t*Bu)][BAr$^F_4$]

To a solution of [Rh(*trans*-PONOP-14)(C_2H_4)][BAr$^F_4$] (10 μmol, generated *in situ*) in DFB (0.5 mL) was added HC≡C*t*Bu (6.0 μL, 48.7 μmol) at RT. The resulting solution was heated at 80 °C for 3 days. Volatiles were removed *in vacuo* and the resulting yellow oil washed with $SiMe_4$ (0.5 mL). Recrystallisation by slow diffusion of $SiMe_4$ into an Et_2O solution at -30 ºC afforded the product was obtained as a yellow crystalline solid. Yield: 6.4 mg (3.97 μmol, 40%).

^{1}H NMR (700 MHz, CD_2Cl_2): *δ* 7.89 (t, $^3J_{HH}$ = 8.1, 1H, py), 7.70–7.74 (m, 8H, Ar^F), 7.56 (br, 4H, Ar^F), 7.31 (d, $^3J_{HH}$ = 15.8, 1H, CH=C<u>H</u>*t*Bu), 6.80 (d, $^3J_{HH}$ = 8.1, 1H, py), 6.79 (d, $^3J_{HH}$ = 8.1, 1H, py), 6.01 (d, $^3J_{HH}$ = 15.8, 1H, C<u>H</u>=CH*t*Bu), 2.60–2.73 (m, 2H, CH_2), 2.41–2.50 (m, 1H, CH_2), 2.13–2.20 (m, 1H, CH_2), 1.75–1.95 (m, 2H, CH_2), 1.68 (s, 9H C≡C*t*Bu), 0.96–1.66 (m, 22H, CH_2), 1.19 (s, 9H, CH=CH*t*Bu), 1.18 (d, $^3J_{PH}$ = 13.8, P*t*Bu), 1.07 (d, $^3J_{PH}$ = 14.0, 9H, P*t*Bu).

^{13}C{^{1}H} NMR (176 MHz, CD_2Cl_2): *δ* 163.5 (d, $^2J_{PC}$ = 3, py), 163.0 (d, $^2J_{PC}$ = 3, py), 162.3 (q, $^1J_{CB}$ = 50, Ar^F), 157.7 (s, CH=<u>C</u>H*t*Bu), 146.9 (s, py), 135.3 (s, Ar^F), 129.4 (qq, $^2J_{FC}$ = 32, $^3J_{CB}$ = 3, Ar^F), 125.1 (q, $^1J_{FC}$ = 272, Ar^F), 118.0 (sept, $^3J_{FC}$ = 4, Ar^F), 115.3 (s, <u>C</u>H=CH*t*Bu), 104.7 (d, $^3J_{PC}$ = 4, py), 104.6 (d, $^3J_{PC}$ = 4, py), 85.7 (d, $^1J_{RhC}$ = 11, C≡<u>C</u>*t*Bu), 68.1 (d, $^1J_{RhC}$ = 12, <u>C</u>≡C*t*Bu), 42.6 (d, $^1J_{PC}$ = 9, P*t*Bu{C}), 41.5 (vt, J_{PC} = 7, P*t*Bu{C}), 35.7 (s, CH=CH<u>*t*Bu</u>{C}), 33.9 (s, C≡C<u>*t*Bu</u>{C}), 32.3 (s, C≡C<u>*t*Bu</u>{CH_3}), 31.9 (d, $^2J_{PC}$ = 3, CH_2), 31.3 (d, $^2J_{PC}$ = 5, CH_2), 30.9 (br, 3×CH_2), 30.7 (s, CH_2), 30.4 (s, CH_2), 30.23 (s, CH_2), 30.22 (s, CH_2), 29.8 (s, CH=CH<u>*t*Bu</u>{CH_3}), 29.63 (s, CH_2), 29.55 (s, CH_2), 29.2 (s, CH_2), 27.7 (d, $^2J_{PC}$ = 6, P*t*Bu{CH_3}), 26.5 (d, $^2J_{PC}$ = 6, P*t*Bu{CH_3}), 24.7 (s, PCH_2), 24.2 (d, $^1J_{PC}$ = 6, PCH_2).

^{31}P{^{1}H} NMR (162 MHz, CD_2Cl_2): *δ* 204.5 (dd, $^2J_{PP}$ = 395, $^1J_{RhP}$ = 140, 1P), 194.5 (dd, $^2J_{PP}$ = 395, $^1J_{RhP}$ = 133, 1P).

HR ESI-MS (positive ion 4 kV): 748.3861 ([*M*]$^+$, calcd 748.3853) *m/z*.

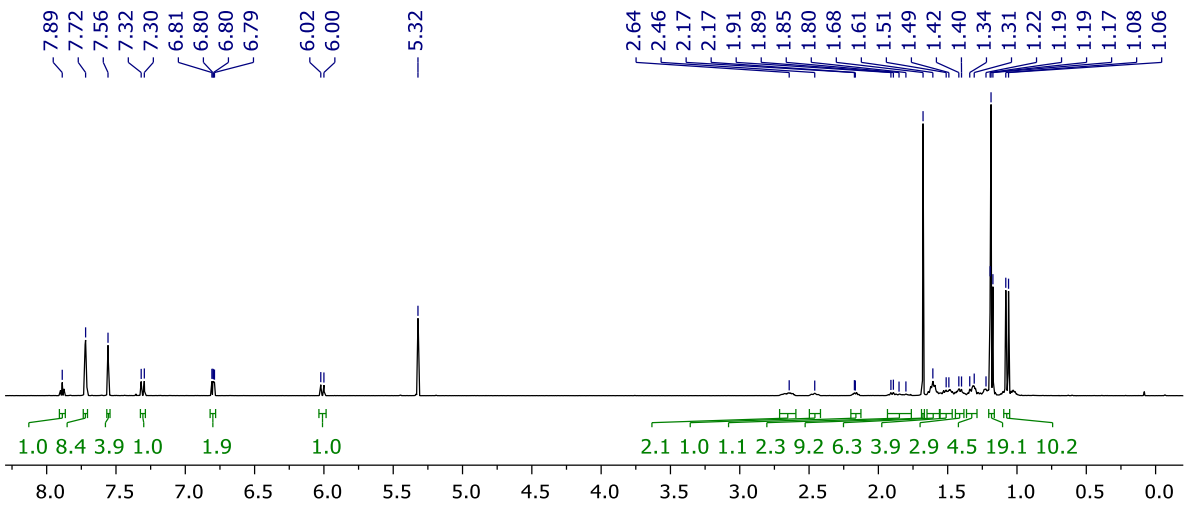

Figure S62. ^{1}H NMR spectrum of [Rh(*trans*-PONOP-14)(*E*-*t*BuC≡CCHCH*t*Bu)][BAr$^F_4$] (CD_2Cl_2, 700 MHz).

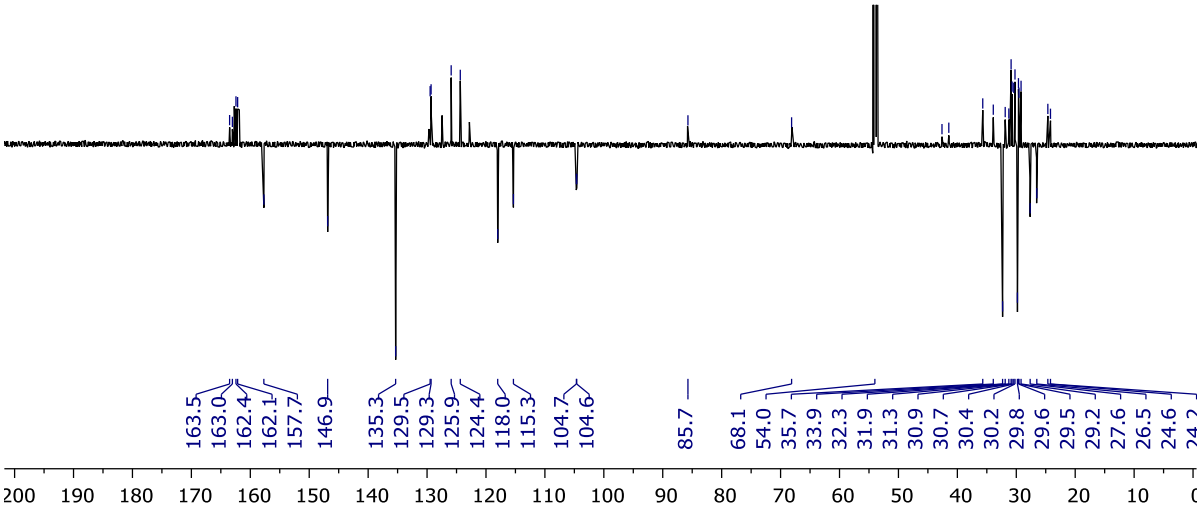

Figure S63. $^{13}C\{^{1}H\}$ APT NMR spectrum of [Rh(*trans*-PONOP-14)(*E*-*t*BuC≡CCHCH*t*Bu)][BAr^{F}_{4}] (CD_2Cl_2, 176 MHz).

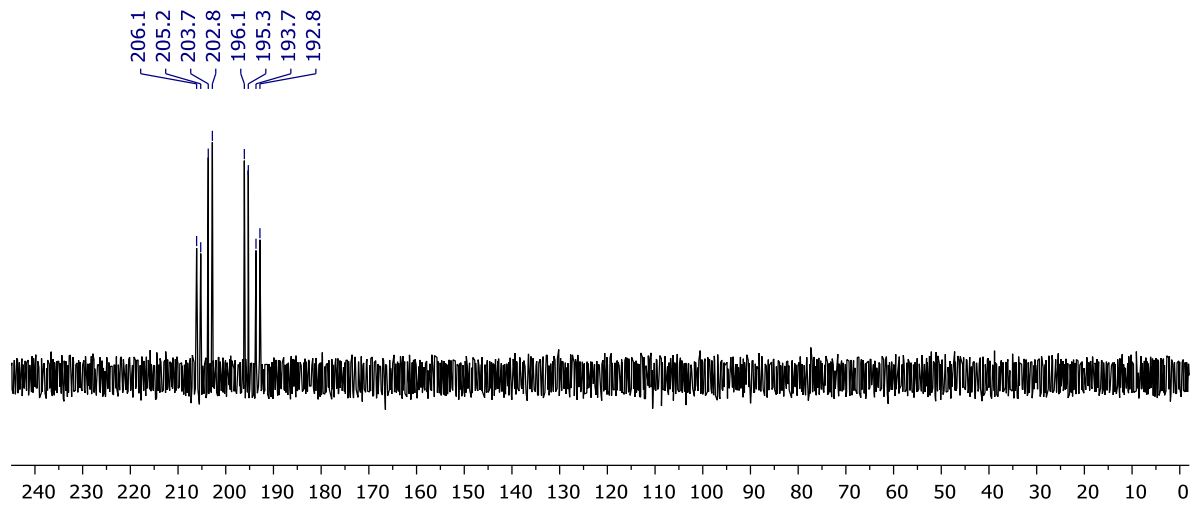

Figure S64. $^{31}P\{^{1}H\}$ NMR spectrum of [Rh(*trans*-PONOP-14)(*E*-*t*BuC≡CCHCH*t*Bu)][BAr^{F}_{4}] (CD_2Cl_2, 162 MHz).

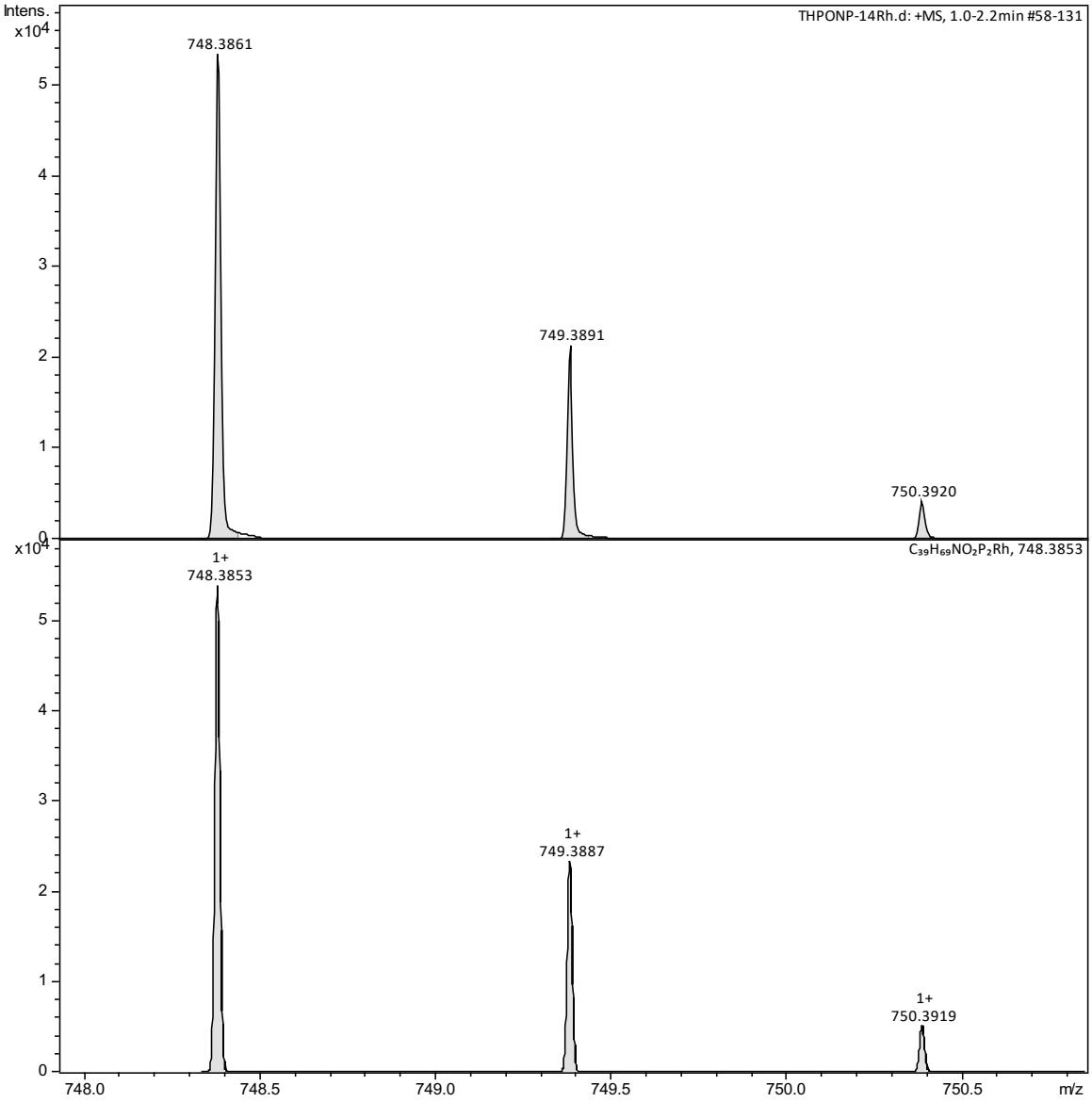

Figure S65. HR ESI-MS of [Rh(*trans*-PONOP-14)(*E*-*t*BuC≡CCHCH*t*Bu)][BAr$^{F}_{4}$].

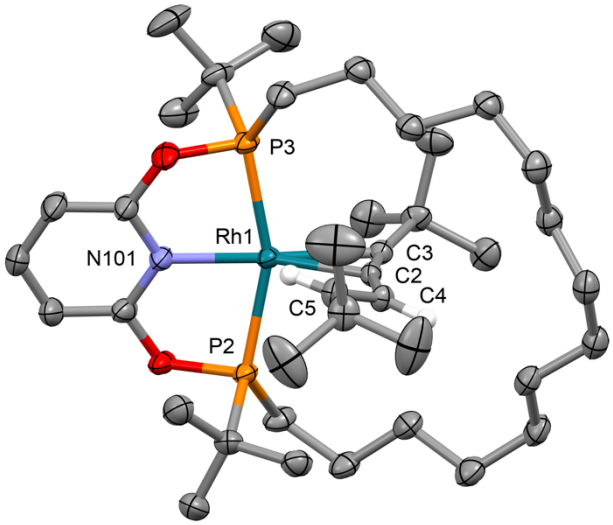

Figure S66. Solid-state structure of [Rh(*trans*-PONOP-14)(*E*-*t*BuC≡CCHCH*t*Bu)][BAr$^{F}_{4}$]: thermal ellipsoids drawn at 50% probability, anion and most hydrogen atoms omitted. Selected bond lengths (Å) and angles (deg): Rh1-P2, 2.3118(10); Rh1-P3, 2.3159(9); Rh1-N101, 2.040(3); P2-Rh1-P3, 158.46(4); Rh1-Cnt(C2,C3), 2.061(2); C2-C3, 1.243(5); C2-C4, 1.447(5); C4-C5, 1.324(5); N101-Rh1-Cnt(C2,C3), 172.22(12); C2-C4-C5, 123.8(4); py-Rh-C≡C twist, 77.1(3) Cnt = centroid.

11. References

1 M. R. Gyton, T. M. Hood and A. B. Chaplin, *Dalton Trans.*, 2019, **48**, 2877–2880.

2 T. M. Hood, M. R. Gyton and A. B. Chaplin, *Dalton Trans.,* 2020, **49**, 2077–2086.

3 E. Neumann and A. Pfaltz, *Organometallics*, 2005, **24**, 2008–2011.

4 A. Bismuto, S. P. Thomas and M. J. Cowley, *Angew. Chem. Int. Ed.*, 2016, **55**, 15356–15359.

5 C. Yang and S. P. Nolan, *J. Org. Chem.*, 2002, **67**, 591–593.

6 E. Negishi, T. Takahashi and K. Akiyoshi, *J. Organomet. Chem.*, 1987, **334**, 181–194